

HRTEM and STEM Image Simulation

CCEM Summer School on Electron Microscopy
at McMaster University
June 5 - 9, 2017

Pierre Stadelmann
JEMS-SAAS
CH-3906 Saas-Fee
Switzerland

June 5, 2017

How to do diffraction/image simulation?

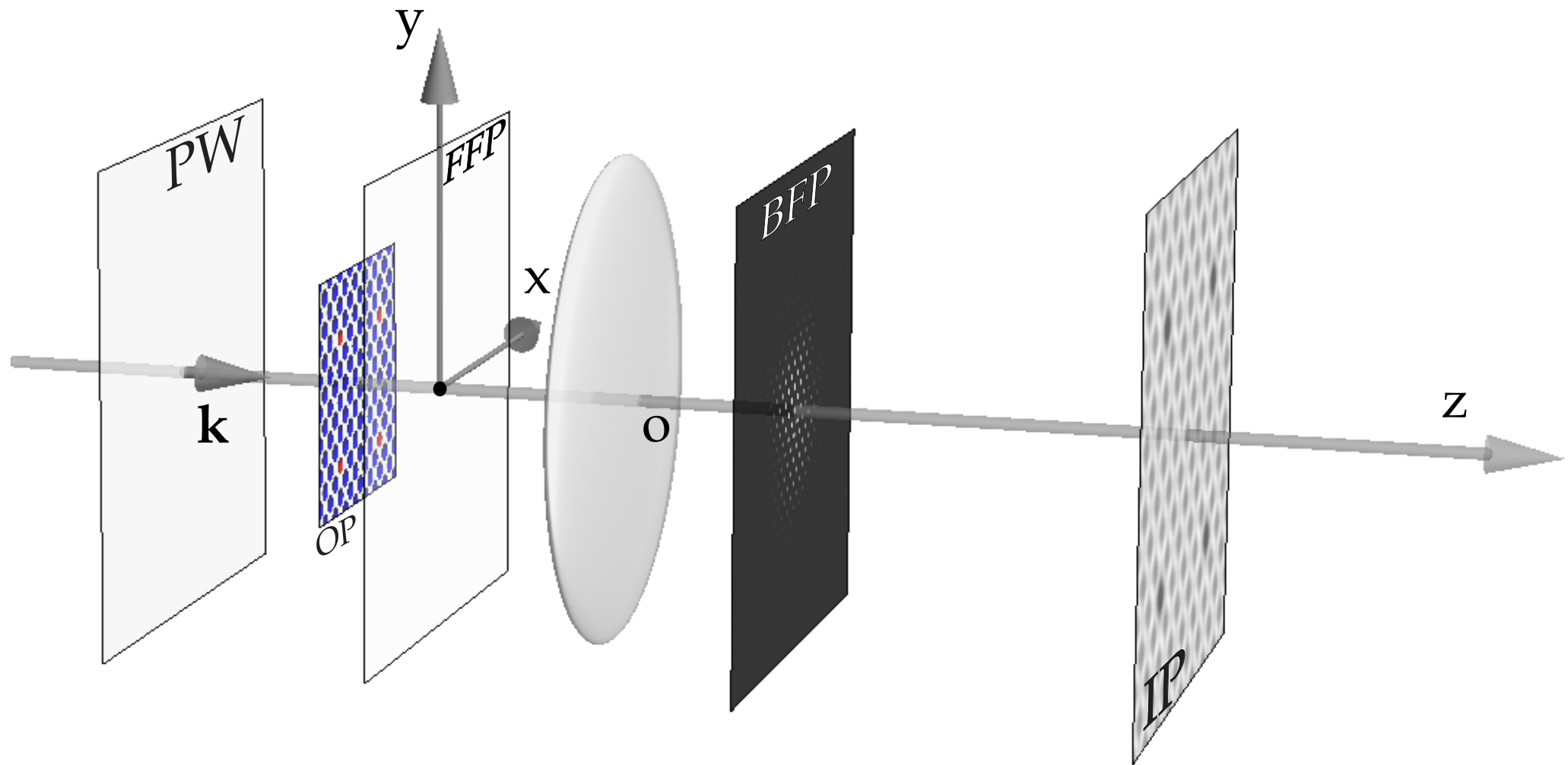
Formation of Electron Microscopy diffraction/images involves complex physical processes.

Approximations and models of these physical processes

are required in order to perform computer simulations. Models are based on electron scattering, diffraction, optics, ...

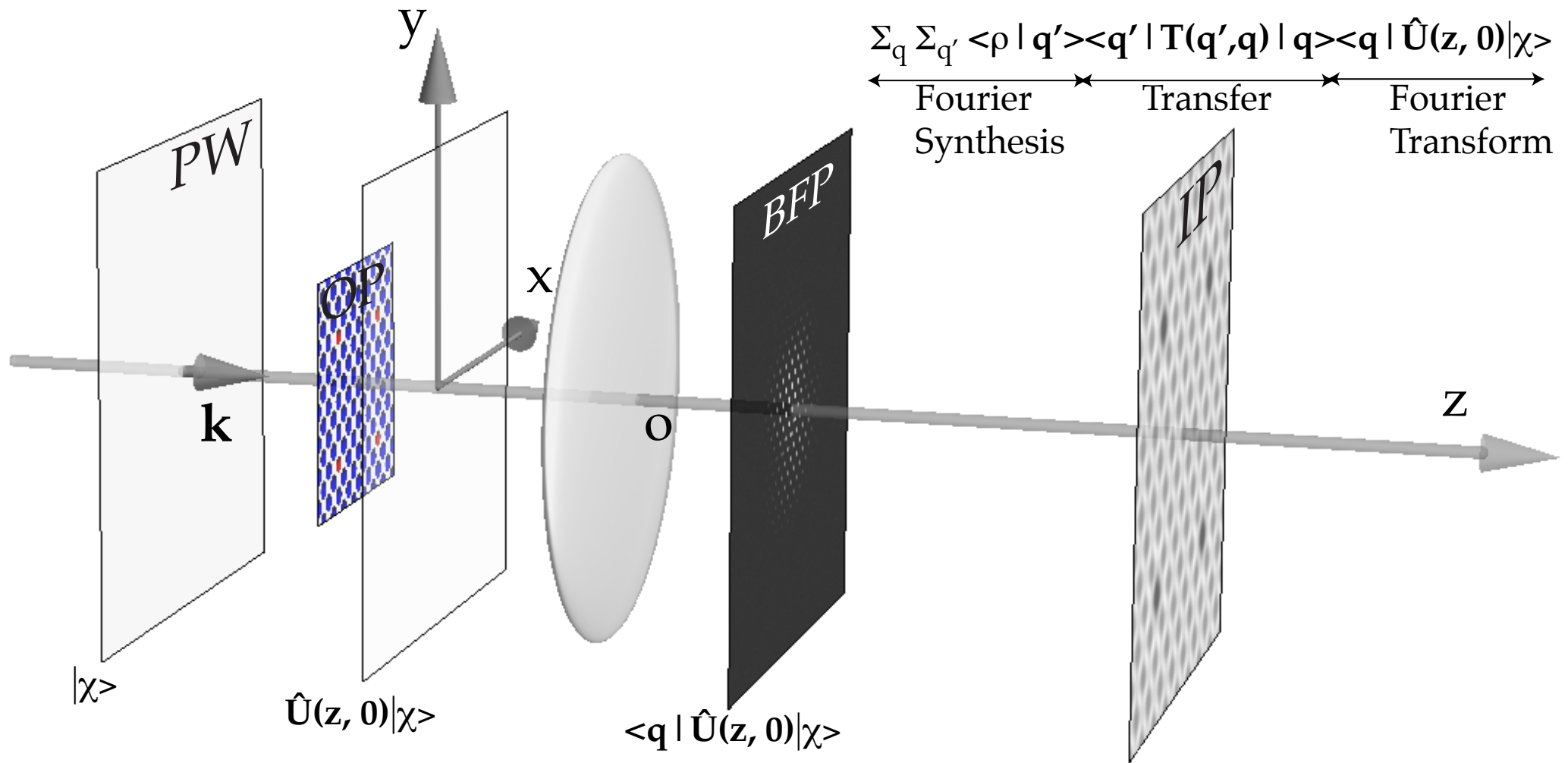
Needed: crystallography, optics, quantum mechanics, ... and computer programming.

TEM (very) simplified model



Modeling steps: Incident wave (PW), crystal (OP), electron-matter interaction, Fraunhofer approximation, image formation (Abbe theory), ...

Image formation modeling (HRTEM)



$|\chi\rangle \implies$ incident wave function

$$|\Psi_i\rangle = \underbrace{\sum_{q'} \langle \rho | q' \rangle}_{\text{Fourier synthesis}} \underbrace{\sum_q \langle q' | T(q', q) | q \rangle}_{\text{Objective lens transfer}} \underbrace{\langle q | U(z, 0) | \chi \rangle}_{\text{Fourier transform}}$$

Assuming that the potential is z independent, the evolution operator $U(z, 0)$ depends on the Hamiltonian $H(\vec{\rho}, z)$ of the system "crystal + incident electron" (where $\vec{\rho}$ are the (x, y) coordinates in a plane perpendicular to the optical axis O_z of the microscope):

$$U(z, 0) = \exp^{-i \int_0^z H(\vec{\rho}, z) dz}$$

The main problem of high-energy electron diffraction and imaging is to determine $U(z, 0)$.

Prior to perform any calculation the following items (from the electron source to the detector) must be characterized and modeled:

- ▶ The electron beam properties.
 - ▶ Convergence.
 - ▶ Source size.
 - ▶ Coherence (spatial and temporal).
- ▶ The specimen properties.
- ▶ How is the incident electron beam scattered by the specimen?
- ▶ How does the microscope transfer the scattered electron beam?
- ▶ How do we measure the properties of the scattered electron beam (diffraction, image, hologram)?
- ▶ What are the properties of the detection system?

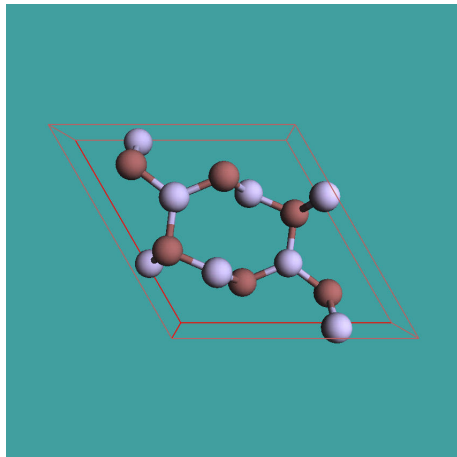
- ▶ Object:
 - ▶ crystal structure.
 - ▶ crystal orientation.
 - ▶ crystal shape.
- ▶ Scattering & Diffraction:
 - ▶ incident wave-function.
 - ▶ evolution operator.
 - ▶ exit wave-function.
- ▶ Image Formation:
 - ▶ HRTEM: Transfer Function (TF) or Transmission Cross Coefficients (TCC).
 - ▶ HRSTEM: Optical Transfer Function (OTF).
- ▶ Image acquisition:
 - ▶ characterisation of the Modulation Transfer Function (MTF) of the detector.

Modelling the object

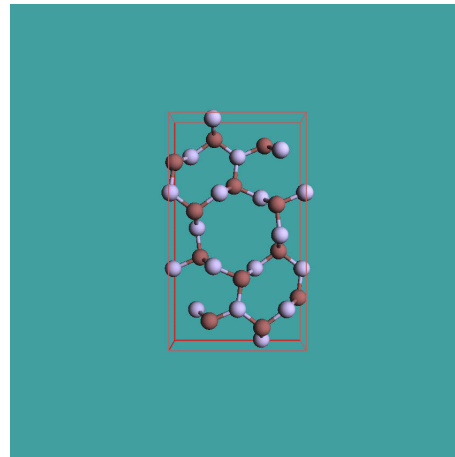
Evolution operator $U(z, 0)$ depends on the object properties

1. Amorphous material or crystalline material.
2. Thin or thick.
3. Orientation (high or low symmetry [uvw]).

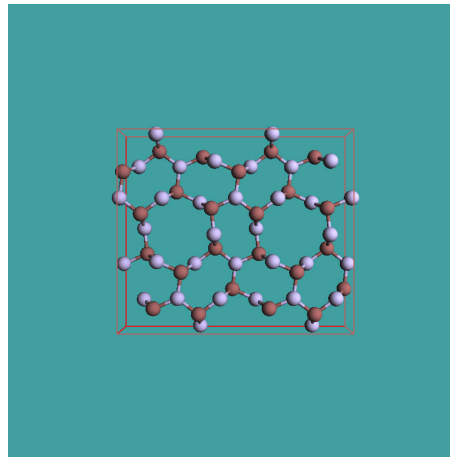
You might have to transform the unit cell in order to perform dynamical calculations¹.



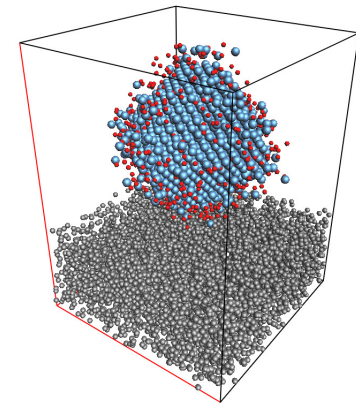
Si_3N_4 hexagonal
lattice.



Si_3N_4 orthorhombic
lattice.



Si_3N_4 orthorhombic
lattice x 2.

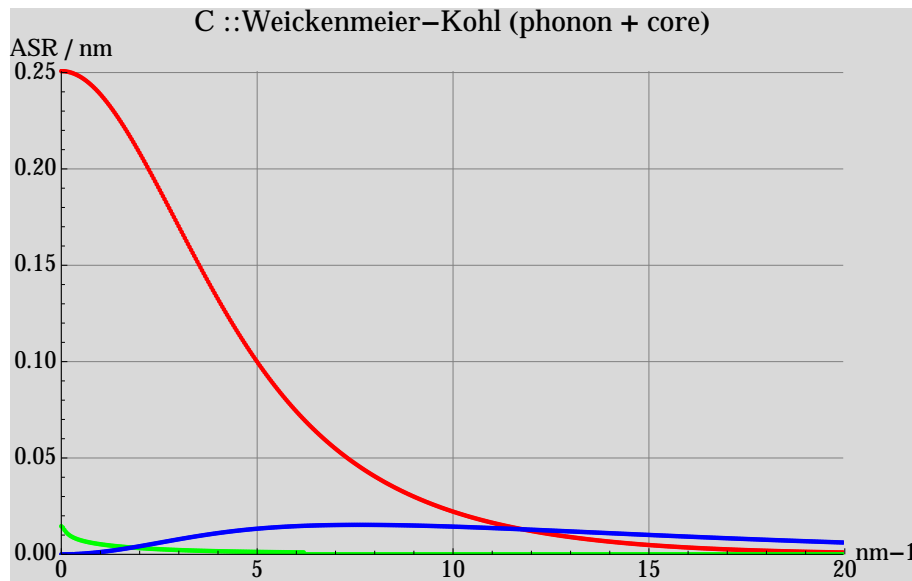


Pt catalyst on
amorphous carbon
film (9600 atoms).

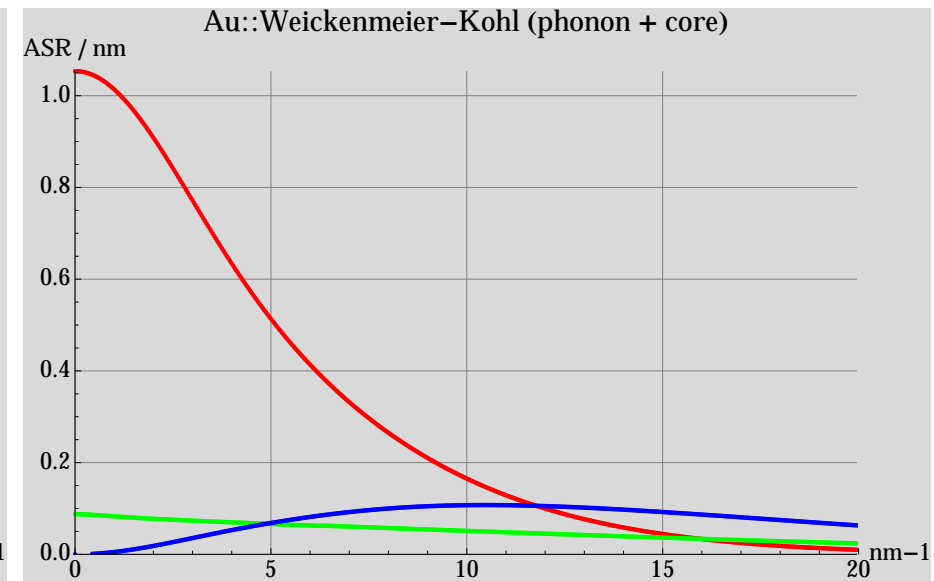
Any model is considered a periodic unit cell independent of its complexity.

¹See International Tables for Crystallography (1992) Vol. 1, Chapter 5.

Atomic scattering amplitude



Carbon. **red**: real part, **green**: imaginary part, **blue**: thermal diffuse scattering.



Gold. **red**: real part, **green**: imaginary part, **blue**: thermal diffuse scattering.

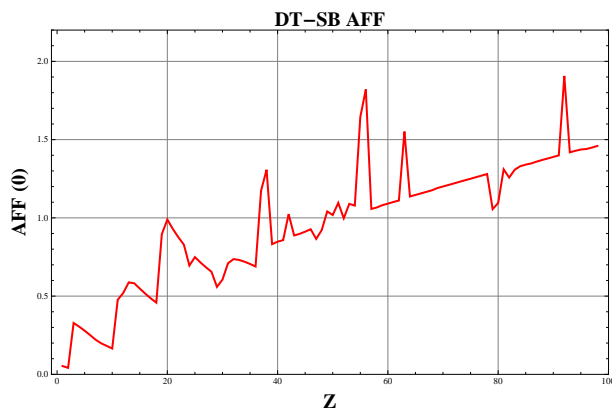
The TDS (**T**hermal **D**iffuse **S**cattering) at large s ($=\sin(\theta)$) scales as $\approx Z^{1.7}$. It explains HAADF (**H**igh **A**nge **A**nnular **D**ark **F**ield) atomic column contrast.

Atomic form factors

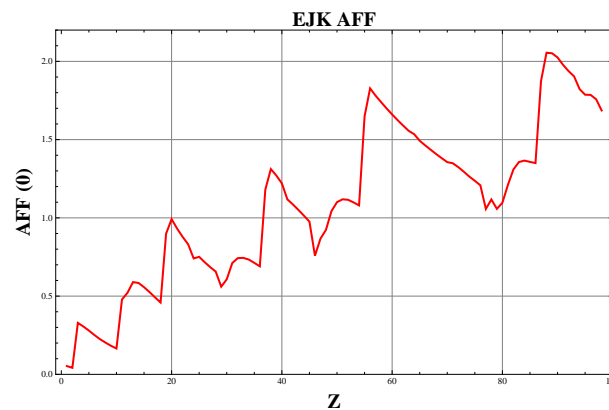
Atomic form factors have been tabulated by many authors:

1. Doyle-Turner and Smith-Burge.
2. E.J. Kirkland.
3. Peng-Ren-Dudarev-Whelan.
4. ...

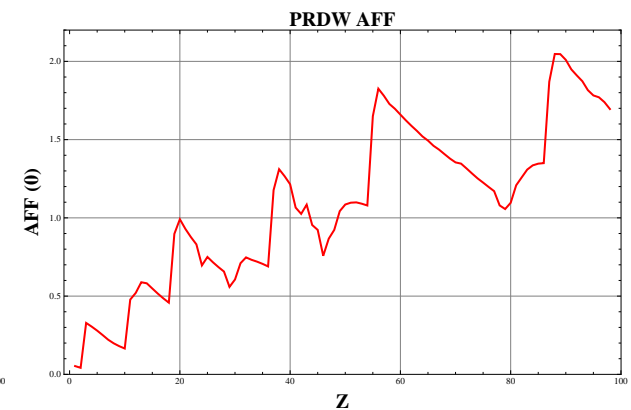
Take care ASA of heavy atoms aren't always tabulated properly.



Doyle-Turner or
Smith-Burger.



E. J. Kirkland.



Peng-Ren-Dudarev-Whelan.

A extremely useful ASA tabulation including phonon and core loss absorption is due to Weickenmeier-Kohl².

²A. Weickenmeier, H. Kohl, Acta Cryst. A 47 (1991) 590.

Crystal structure are defined by:

1. $a, b, c, \alpha, \beta, \gamma$ lattice parameters.
2. Space-group or symmetry operators.
3. Atoms positions (Symbol, x, y, z with $0 \leq (x, y, z) < 1$)

$> 10^5$ crystal structures provided by data bases (ICSD, Min. Soc. Ame., Cryst. Open Database).

Useful servers:

www.minsocam.org

www.crystallography.net

www.cryst.ehu.es

ICSD & AMS: data bases for crystal structures

Available CIF files

- Triiron tetraoxide
- Iron oxide (0.93/1)
- Iron oxide
- Iron(III) oxide - alpha
- Iron(III) oxide - alpha
- Iron(III) oxide - alpha
- Iron(III) oxide - alpha
- Iron(III) oxide - alpha
- Iron(III) oxide - alpha
- Iron oxide (2.93/4)
- Iron oxide (2.95/4)
- Iron oxide (2.94/4)
- Iron oxide (2.95/4)
- Iron oxide (2.94/4)
- Iron oxide (2.94/4)
- Iron oxide (2.94/4)
- Iron oxide (2.96/4)
- Iron oxide (2.96/4)
- Iron oxide (2.94/4)
- Iron oxide (2.95/4)
- Iron(III) oxide - alpha
- Iron oxide (21.34/32) - gamma
- Iron diiron(III) oxide
- Iron(III) oxide - alpha
- Iron(III) oxide - alpha
- Iron oxide (.92/1)
- Iron oxide (.93/1)
- Iron oxide (.89/1)
- Iron oxide (.91/1)
- Iron oxide (.91/1)
- Iron oxide (0.95/1)
- Iron(III) oxide - alpha
- Iron oxide
- Triiron tetraoxide
- Iron oxide (0.93/1)
- Iron(III) oxide - alpha
- Iron(III) oxide - alpha
- Iron(III) oxide - alpha
- Iron(III) oxide - alpha
- Iron oxide (2.93/4)
- Iron oxide (2.95/4)
- Iron oxide (2.93/4)
- Iron oxide (2.94/4)
- Iron oxide (2.93/4)
- Iron oxide (2.94/4)
- Iron oxide (2.93/4)
- Iron oxide (2.94/4)
- Iron oxide (2.96/4)
- Iron oxide (2.96/4)
- Iron oxide (2.94/4)
- Iron oxide (2.95/4)
- Iron(III) oxide - alpha
- Iron(III) oxide - alpha
- Iron(III) oxide - alpha
- Iron oxide (.92/1)
- Iron oxide (.88/1)
- Iron oxide (.9/1)
- Iron oxide (.92/1)
- Iron oxide (0.95/1)
- Diiron(III) oxide - alpha

Cancel Select

Fe (0) at : (0.375, 0.375, 0.875)

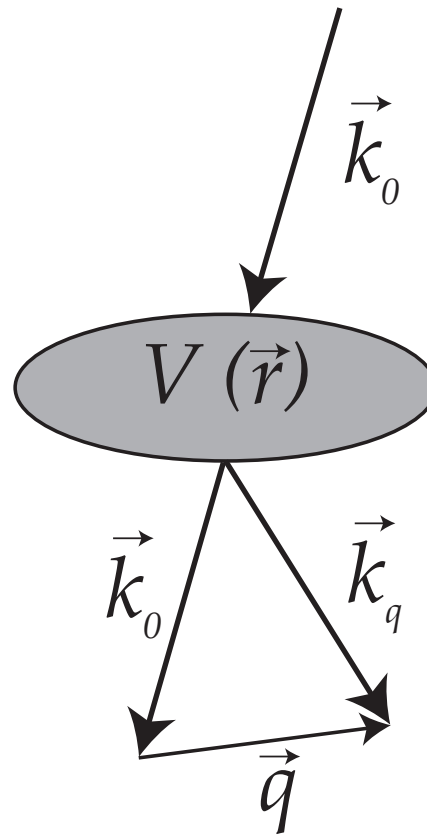
ICSD_82237 : [0, 0, 1]

Projections

- [0, 0, 1]
- [1, 0, 0]
- [0, 1, 0]

Scattering & diffraction

Scattering: electron-matter interaction

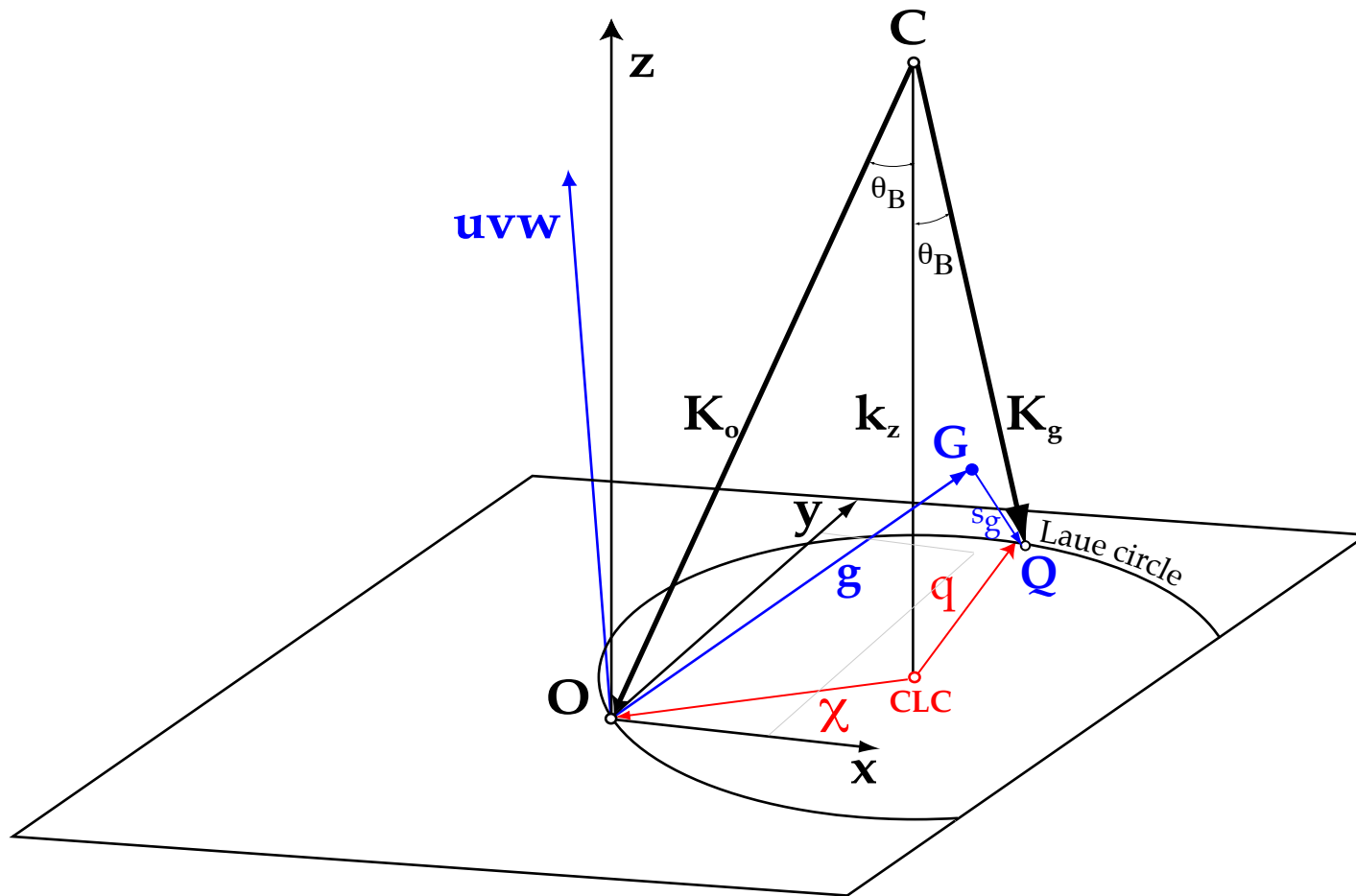


An incident electron of wave vector \vec{k}_0 interacts with a solid of scalar potential $V(\vec{r})$. The wave vector of the scattered electron is $\vec{k}_q = \vec{k}_0 + \vec{q}$ where \vec{q} is the momentum transferred by the solid³.

Elastic scattering $\longrightarrow ||\vec{k}_q|| = ||\vec{k}_0||$.

³Magnetic and spin effects are ignored.

Diffraction geometry: small angle approximation



Center of the Ewald sphere (C) and Center of the Laue Circle (CLC), projection of C onto the zero order Laue zone. All reflections on the circle of radius χ are at exact Bragg condition. Notice that the Bragg angles are **pretty small** (of the order a few $^\circ$) and that consequently the **small angle approximation** is quite good.

Kinematical diffraction: $\langle q|U(z,0)|\chi\rangle$

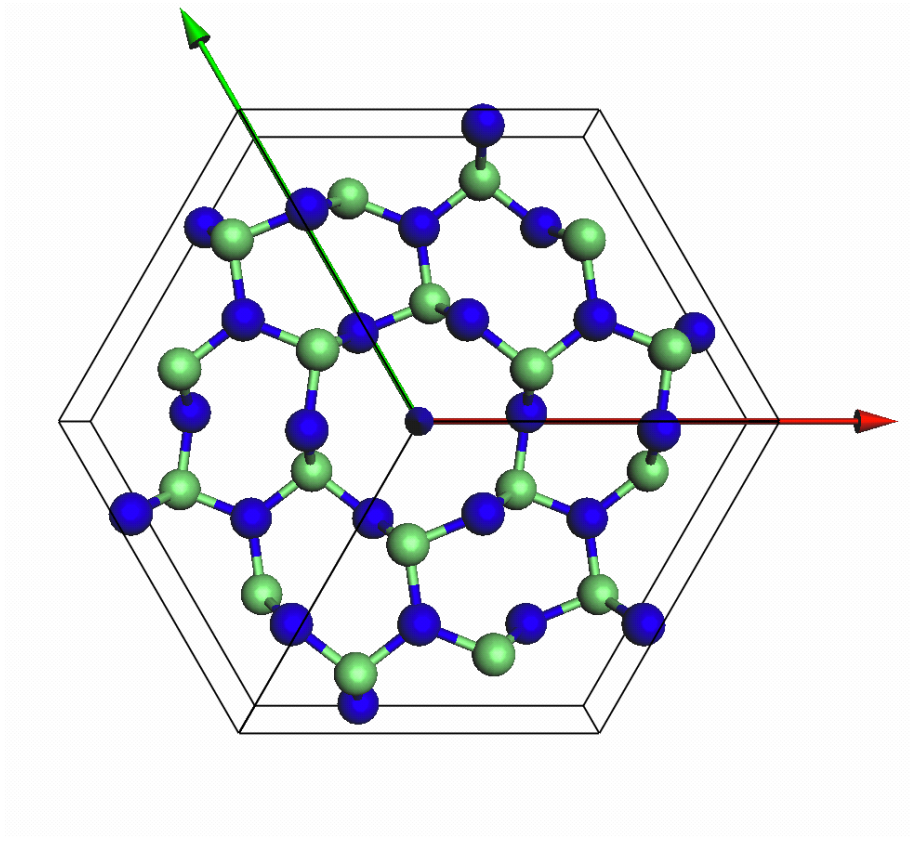


Figure: Model (Ge_3N_4).

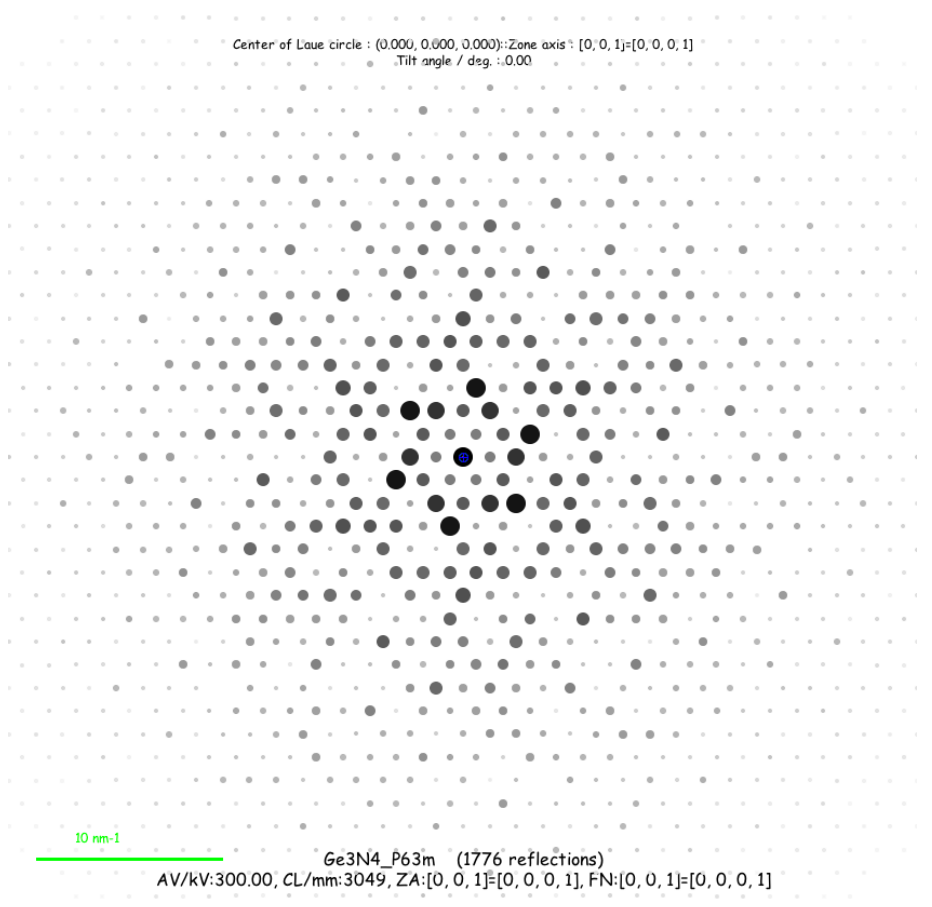


Figure: Kinematical diffraction Ge_3N_4 , [001].

Kinematical diffraction assumes single scattering approximation, i.e. very thin crystals.

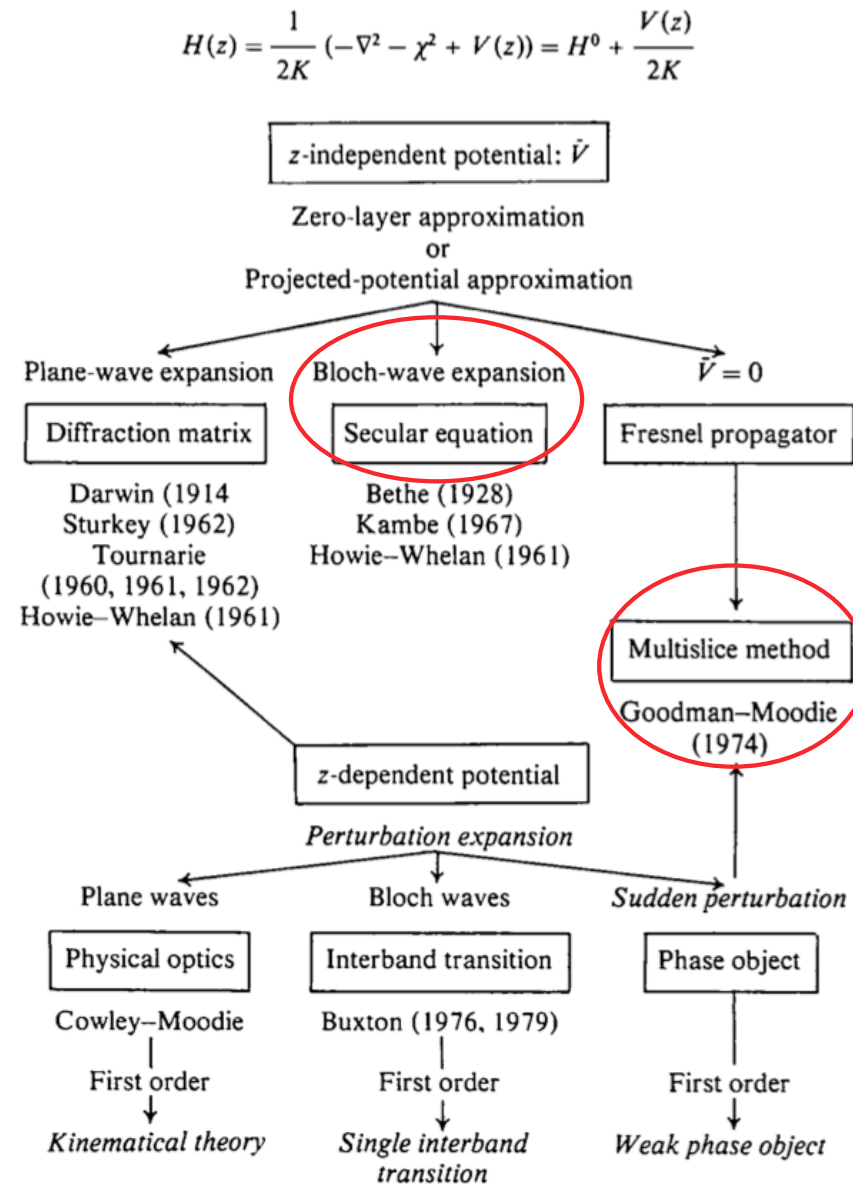
Dynamical scattering or multiple scattering models the fact that electrons suffer multiple scattering events passing through the crystal slab. It is mathematically modelled as:

$\langle q|U(z,0)|\chi \rangle \implies$ Fourier transform of object wavefunction

Dynamical scattering (many different approaches under small angle approximation and elastic scattering). Including inelastic scattering gives more complicated and computer intensive calculations.

One must read paper!

Gratias & Portier: small angle & elastic scattering approximations



From Gratias and Portier⁴.

⁴D. Gratias and R. Portier, Time-Like Perturbation Method in High-Energy Electron Diffraction, Acta Cryst. **A39** (1983) 576-584

The two most employed calculation methods

All approximations are numerically equivalent, but perform best in particular cases.

We will consider only 2 approximations:

- ▶ multislice approximation⁵.
- ▶ The Bloch-wave method⁶.

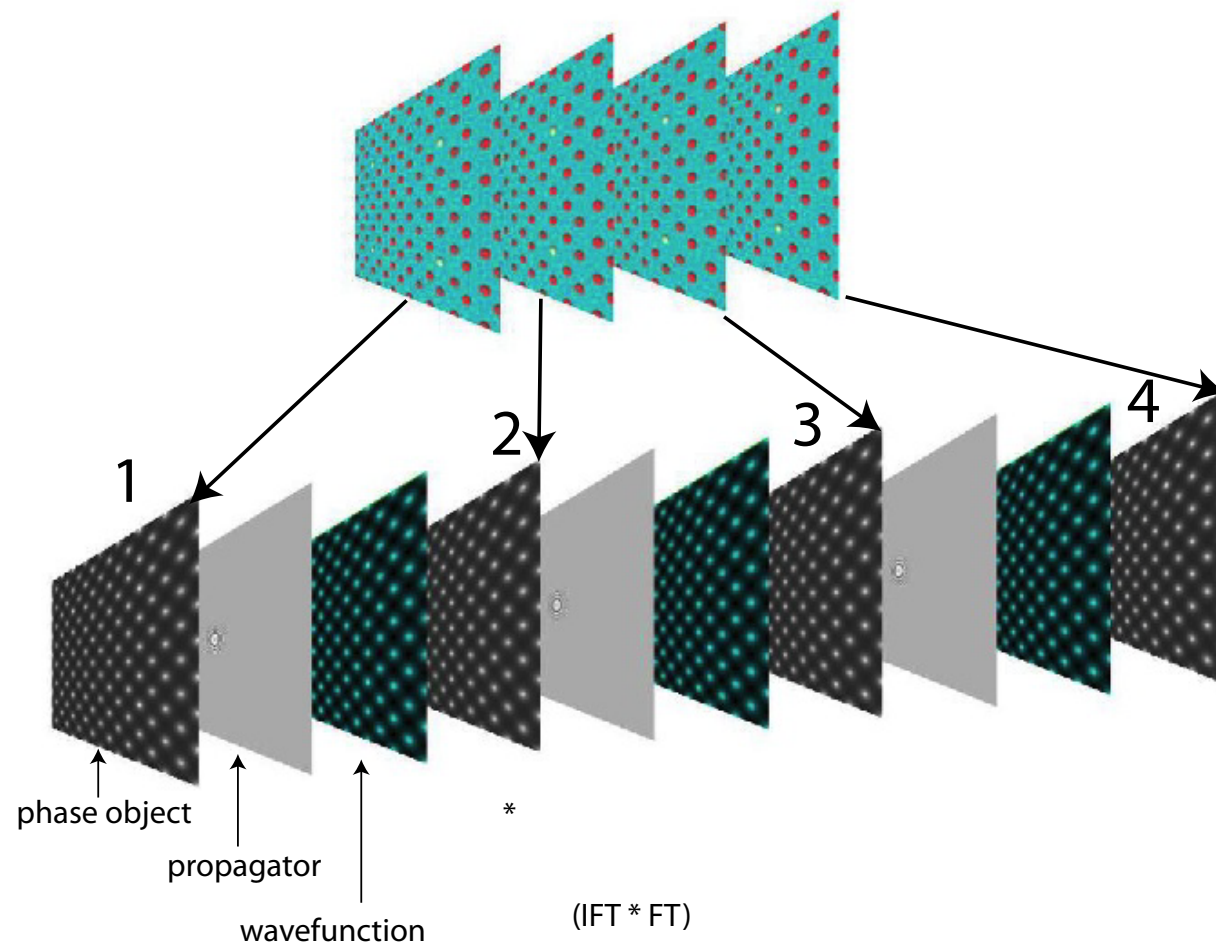
The **multislice** method models multiple scattering within the context of physical optics⁷. It performs best when simulating crystalline or amorphous solids of large unit cell or containing defects while the **Bloch-wave** method is adapted to the calculation of crystalline solids of small unit observed in any [uvw] orientation. The Bloch-wave method has also several advantages (speed, ease of use) for simulating CBED, LACBED or PED patterns and for polarity and chirality determination.

⁵J. Cowley and A.F. Moodie, Proc. Phys. Soc. B70 (1957) 486, 497 and 505.

⁶H. A. Bethe, Ann. Phys. 87 (1928), 55.

⁷J.W. Goodman, Introduction to Fourier Optics, McGraw-Hill, 1968.

Multislice method



The solid is sliced into thin sub-slices. The incident wave-function is transferred by the first slice (diffraction) and propagated to the next one. The propagation is done within the Fresnel approximation, the distance between the slices being 20 - 50 times the wavelength.

$$\Psi(i+1) = [\Psi(i)PO(i)] \otimes FP_{i \rightarrow i+1}$$

Multislice algorithm

2 steps:

- ▶ Diffractor: transfer by one slice \Rightarrow multiplication by phase object function ($POF(\vec{\rho})$).
- ▶ Propagator: propagation between slices \Rightarrow convolution by the Fresnel propagator (is nowadays performed by a FFT followed by a multiplication and an inverse FFT (FT^{-1} , multiplication, FFT)) (calculation error $O(z)$).

For improved multislice calculations ($O(z^2)$) the wave-function is propagated over $z/2$, then multiplied by the phase-object function of the slice and finally propagated again over $z/2$. Slices do not need to have equal thicknesses.

Work best to simulate:

- ▶ Perfects crystals of large unit cell parameters⁸.
- ▶ Defects under the periodic continuation assumption⁹.

Is also used for:

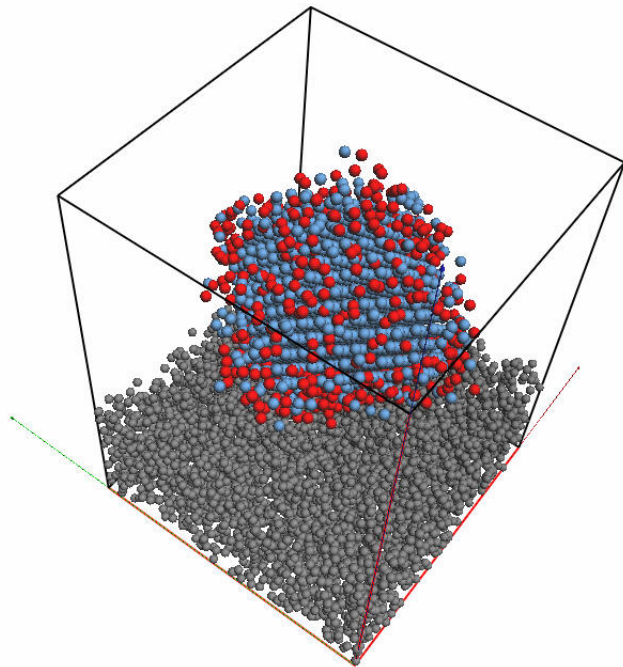
- ▶ ADF image simulation in the "Frozen Lattice" approximation¹⁰.

⁸K. Ishizuka, Acta Cryst. A33 (1977) 740-749.

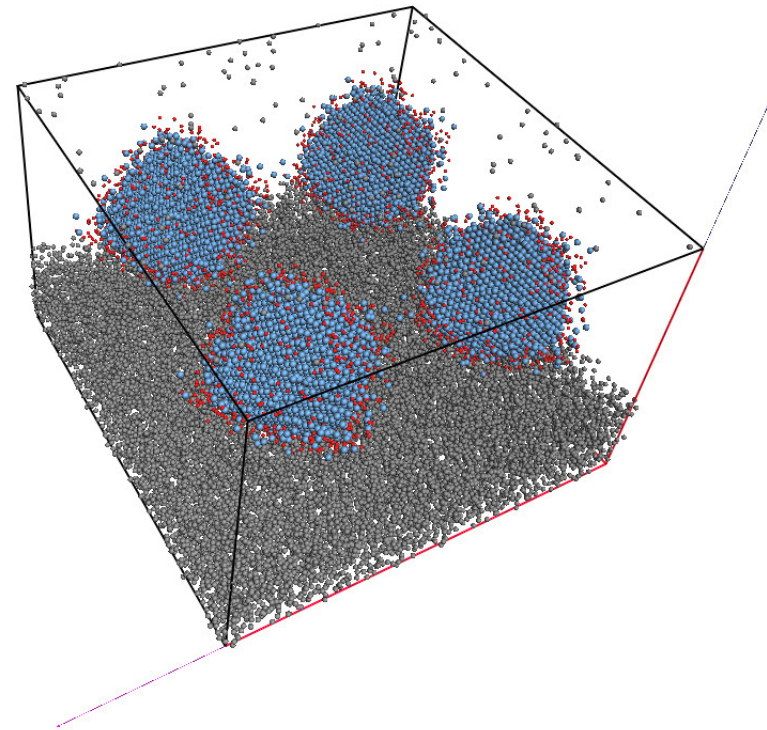
⁹A.J. Skarnulis, Thesis, Arizona State University 1975.

¹⁰E.J. Kirkland, *Advanced Computing in Electron microscopy*.

Multislice: periodic continuation



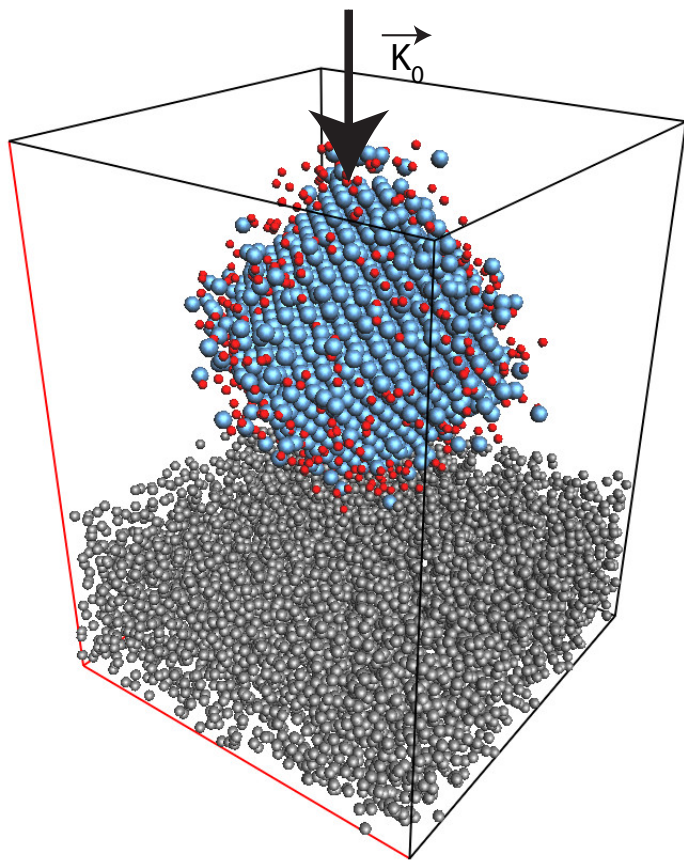
One unit cell model.



Periodic continuation model (2 x 2 unit cells).

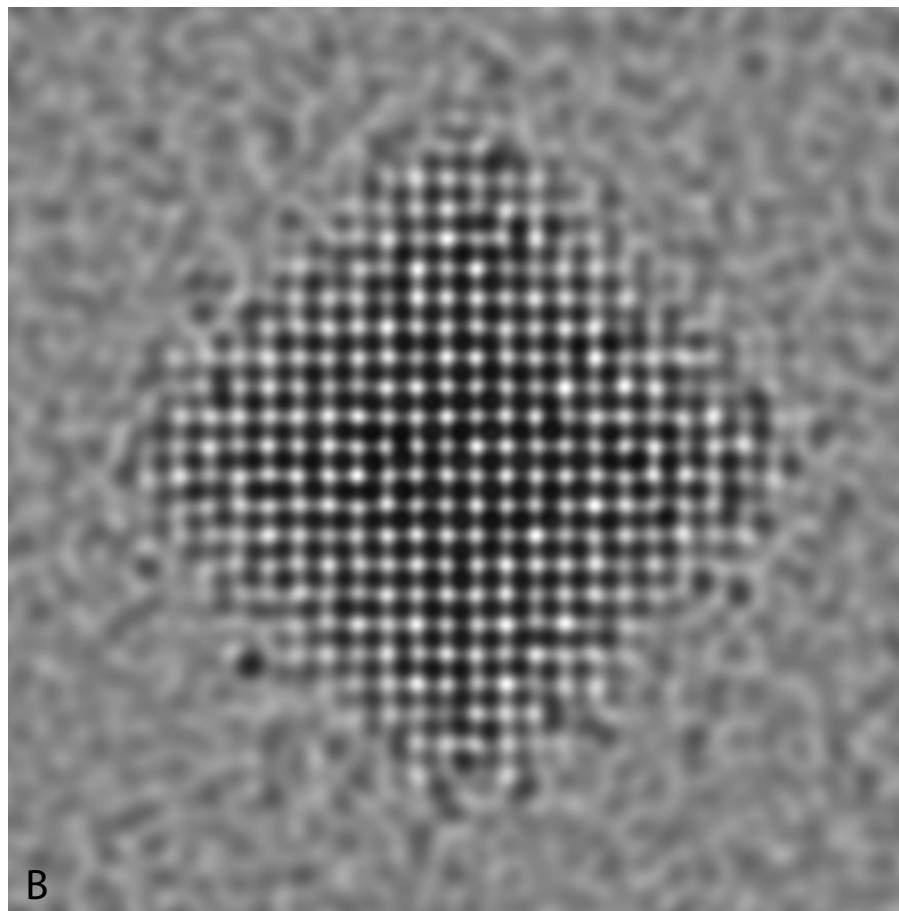
In order to avoid "aliasing problems" during the multislice iterations the phase-object function and the propagator function must be sampled properly and also be "band-limited".

Example multislice: Pt catalyst



A

A: catalyst model (9500 atoms)



B

B: HREM image (Jeol 400kV).

This simulation was performed with a phase-object function sampled on a 1024 x 1024 grid.

Bloch wave method: z-independent potential

When the scattering potential is periodic, the eigenstates $|j\rangle$ of the propagating electrons are Bloch waves. The hamiltonian of the system is projected on the eigenstates $|j\rangle$ with eigenvalues γ_j ("anpassung" parameter).

$$\hat{H} = \sum_j \gamma_j |j\rangle \langle j|$$

The evolution operator is then given by (since $V = V(\vec{\rho})$):

$$\hat{U}(z, 0) = e^{-i\hat{H}z} = \sum_j e^{-i\gamma_j z} |j\rangle \langle j|$$

The wave-function at z developed on plane waves basis $|q\rangle$:

$$\Psi(z) = \sum_q \phi_q(z) |q\rangle$$

$$\phi_q(z) = \langle q | \hat{U}(z, 0) | 0 \rangle = \sum_j e^{-i\gamma_j z} \langle q | j \rangle \langle j | 0 \rangle$$

$$c_0^{*j} = \langle j | 0 \rangle \quad \text{and} \quad c_q^j = \langle q | j \rangle$$

where in usual notation c_0^{*j} and c_q^j are the Bloch-wave excitations (component of the initial state $|0\rangle$ on $|j\rangle$) and coefficients (component of reflection $|q\rangle$ on $|j\rangle$) respectively¹¹.

¹¹C. Humphreys & R.M. Fisher, Bloch Wave Notation in Many-Beam Electron Diffraction, Acta Cryst. **A27** (1971) 42-45.

Simulation of:

- ▶ SAED (kinematical and dynamical).
- ▶ CBED (polarity).
- ▶ LACBED (specimen thickness, symmetry).
- ▶ PED (Precession Electron Diffraction).
- ▶ HRTEM.

Works best for small lattice parameters crystals¹².

¹²Some more details in Appendix1.

CBED: ZnTe [110]

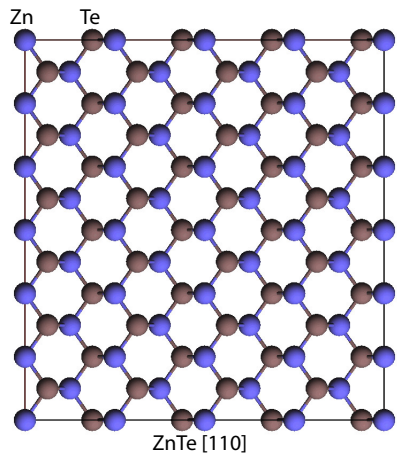


Figure: ZnTe [110].

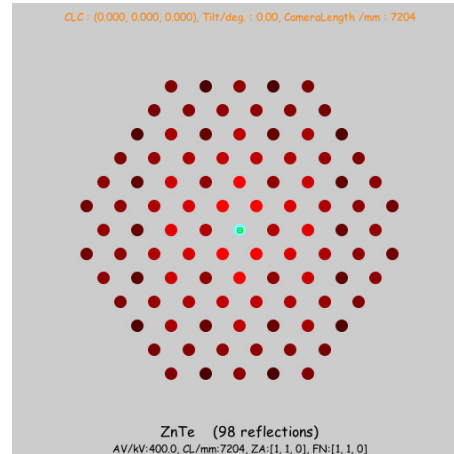


Figure: Reflections (1 + 49), $|\chi| \geq 0$.

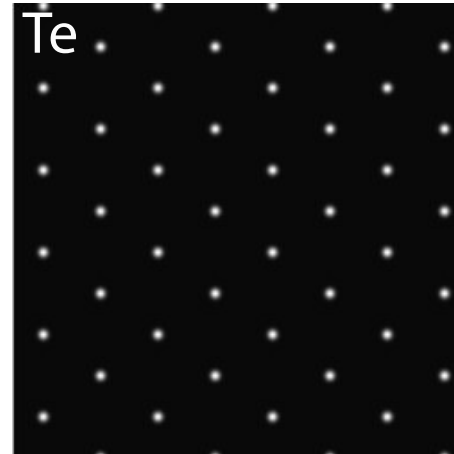


Figure: Bloch-wave 1 (Te 1s).

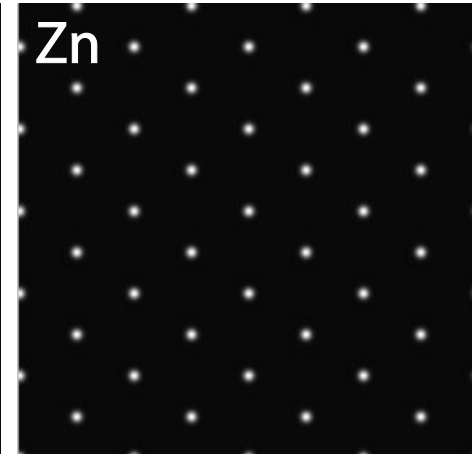


Figure: Bloch-wave 2 (Zn 1s).

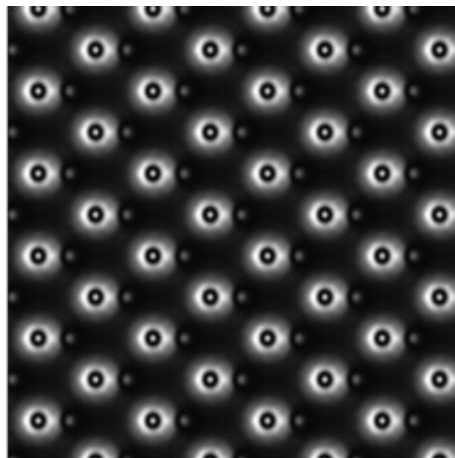


Figure: Bloch-wave 5 (Te-Zn).

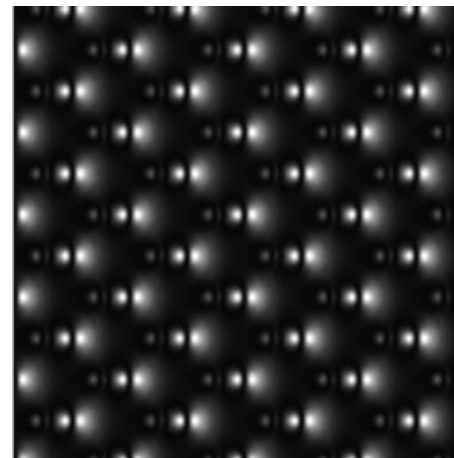


Figure: Bloch-wave 7 (Te-Zn).

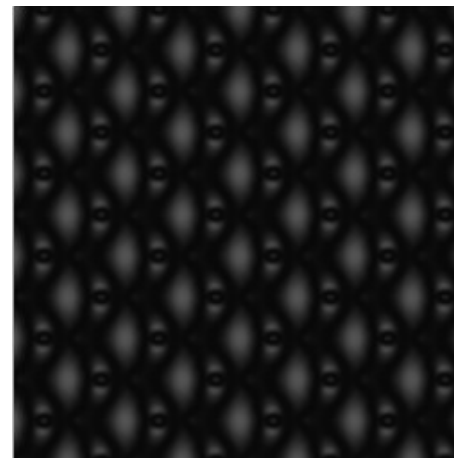


Figure: Bloch-wave 8 (Te-Zn).

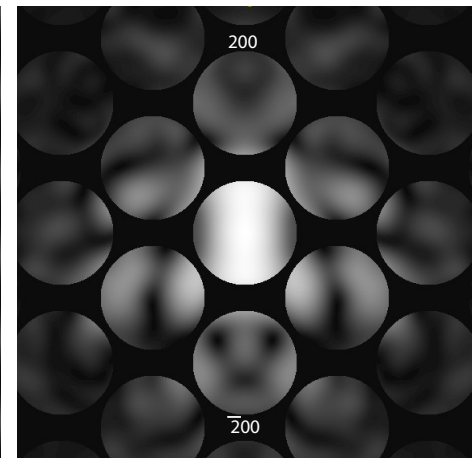
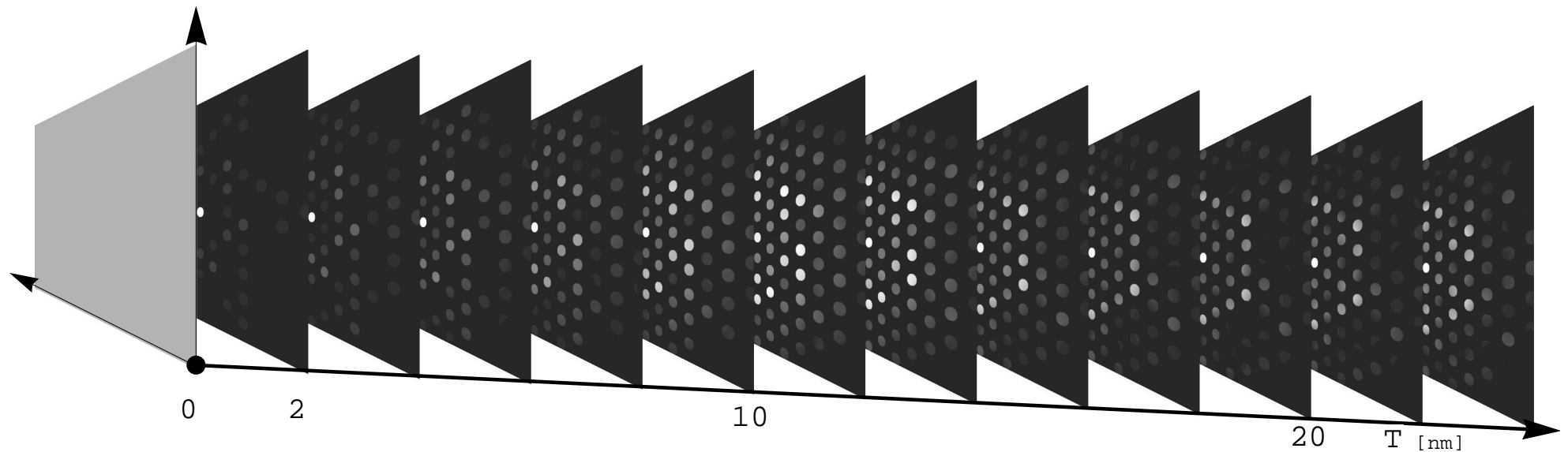


Figure: CBED (ZnTe polarity).



In BFP diffraction pattern depends specimen thickness.

Goodness of dynamical diffraction theories?

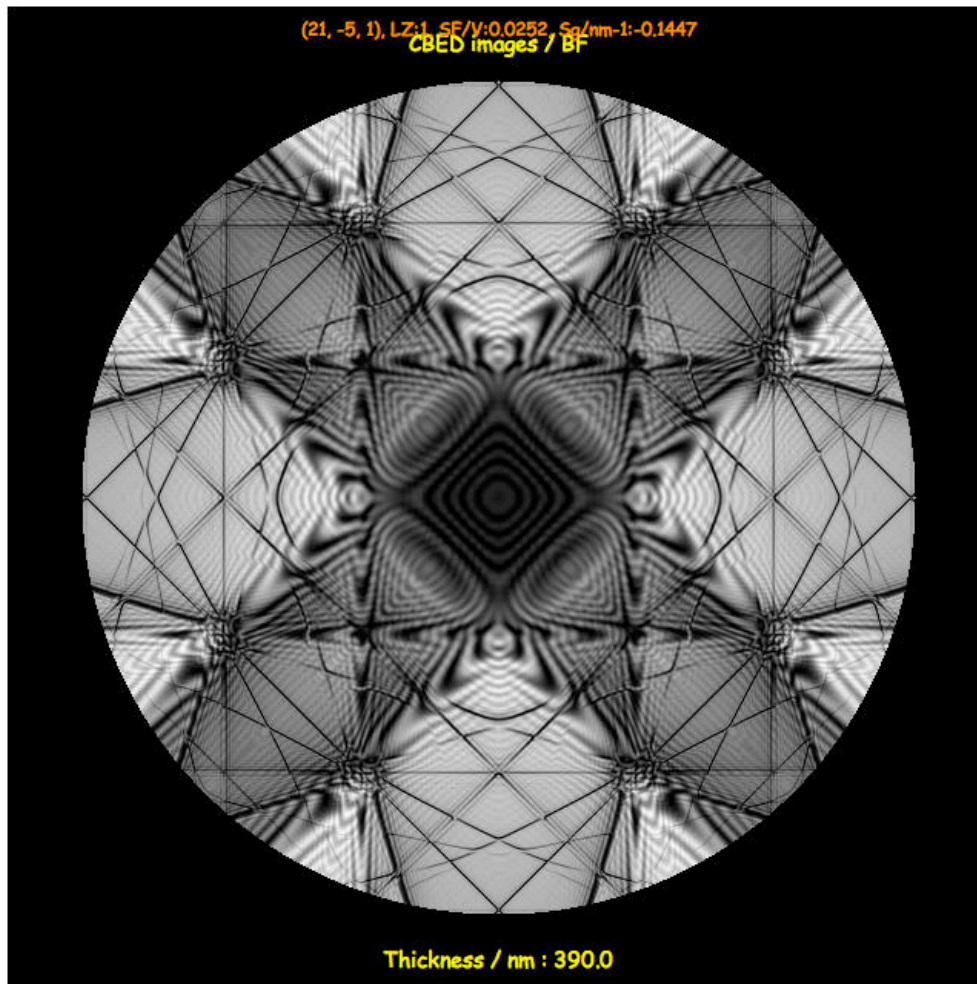


Figure: LACBED Si [001]: simulation.

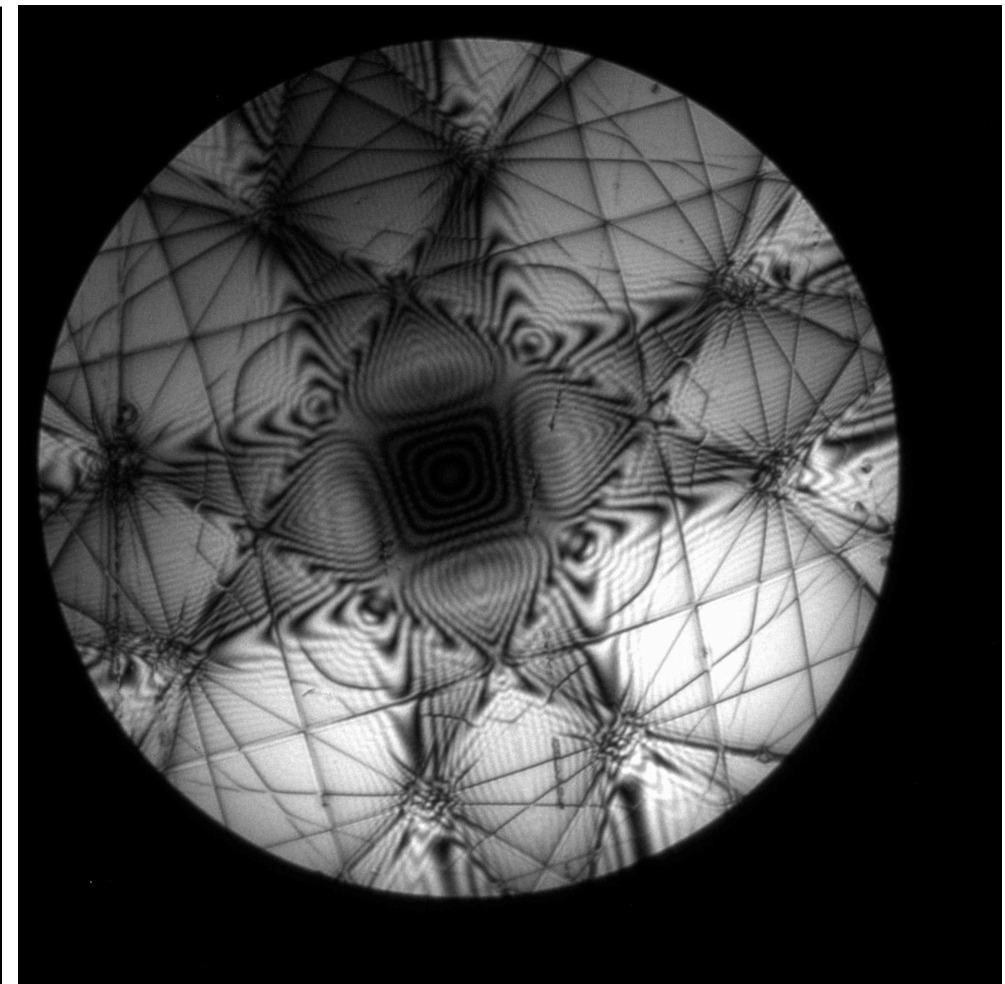


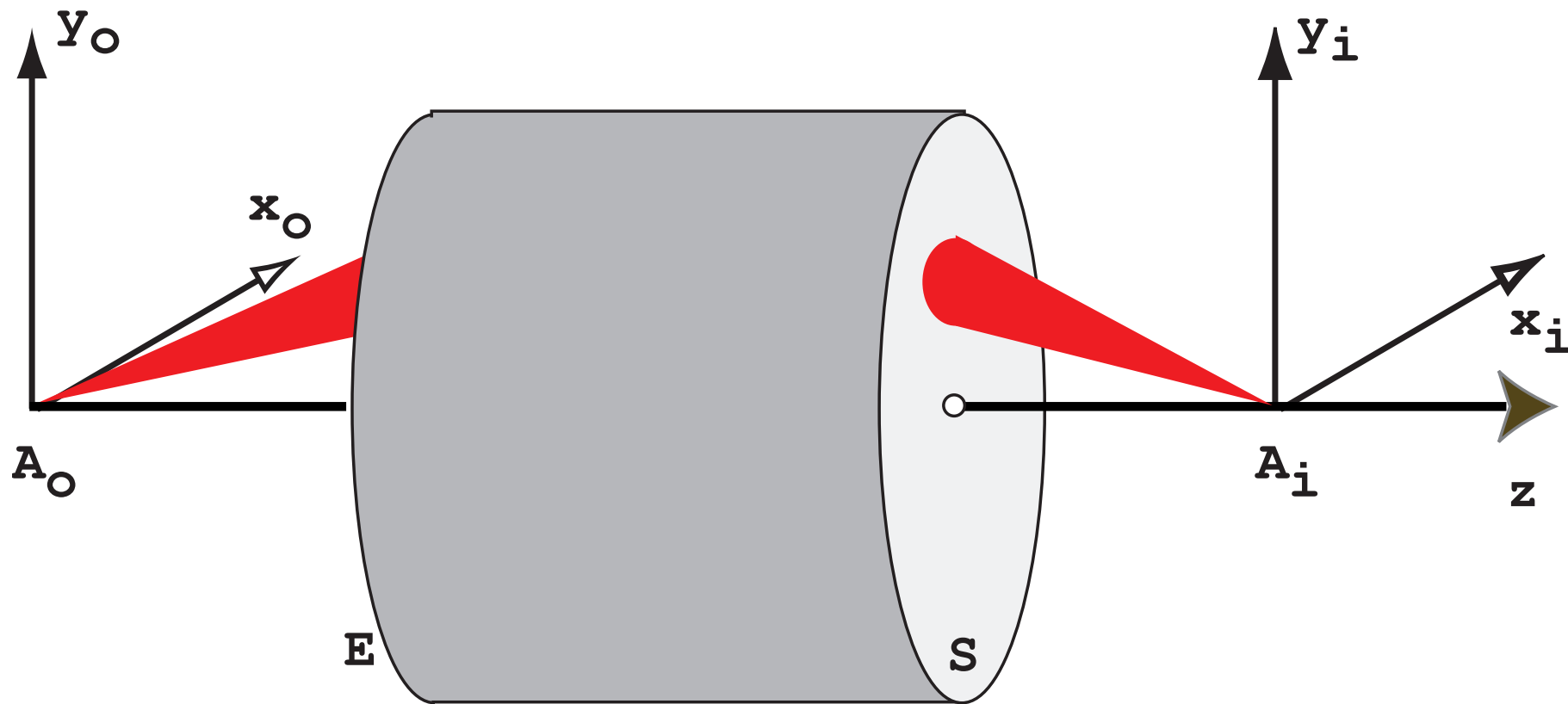
Figure: LACBED Si [001]: experimental (Web site EM centre - Monash university, J. Etheridge).

Note that the experimental LACBED pattern is blurred (inelastic scattering and/or MTF of CCD camera?).

Image formation

- ▶ Abbe image formation.
- ▶ Transfer function.
- ▶ Perfect thin lens.
- ▶ Aberrations.

Optical system



An optical system produces the **image** A_i of a **point source** object A_o . A_o and A_i are said to be conjugate. A_i is **not** a point since any optical system is diffraction limited. This limitation is introduced by the entrance and exit pupils of the optical system.

Some light rays emitted by object point A_o do not reach the image at point A_i .

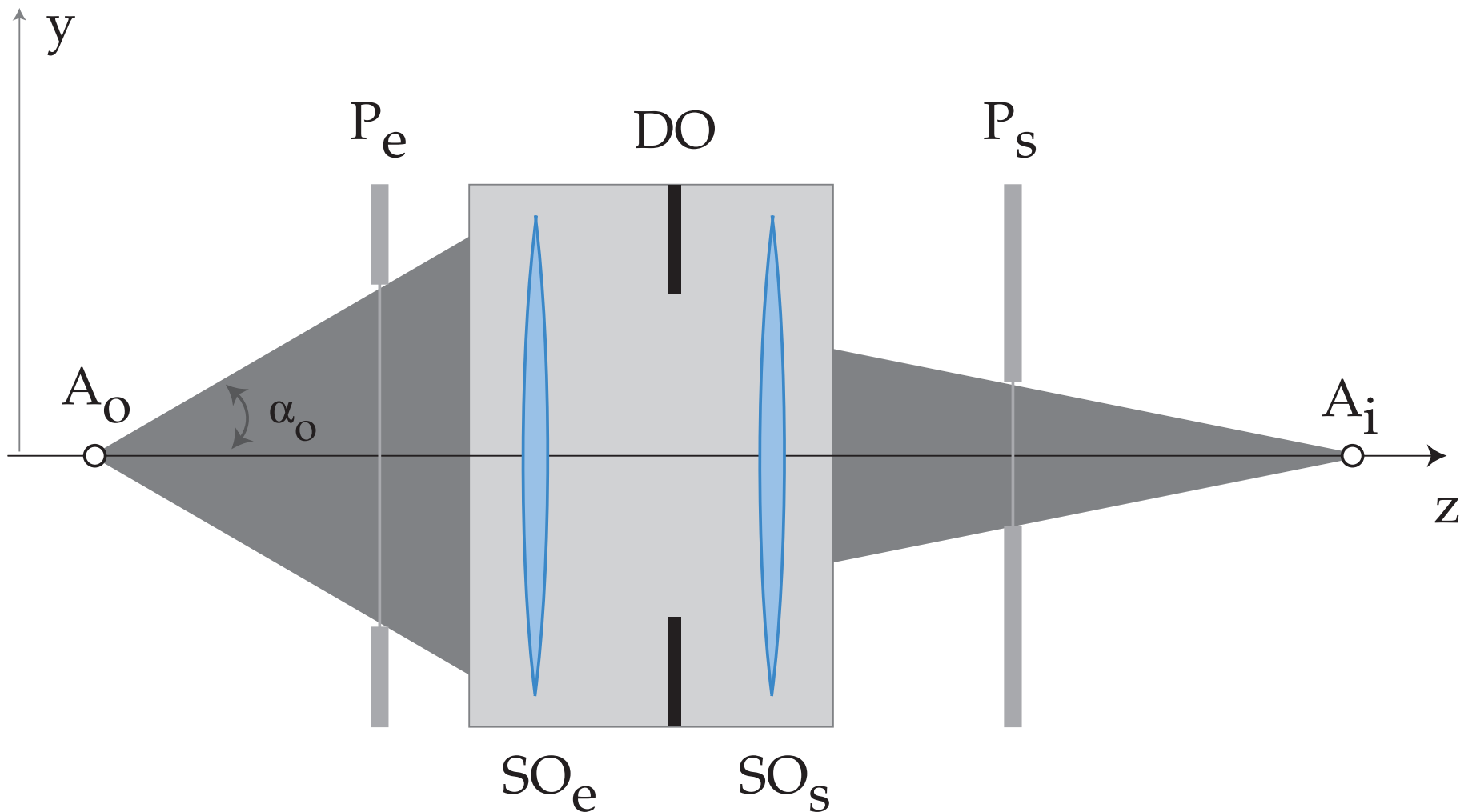
Position of A_i \longrightarrow intersection of the reference light ray (non deviated) and the image plane.

The image of a point source is a **spot** whose shape and intensity depend of the quality of the optical system.

Two types of aberrations:

1. **Monochromatic.**
2. Chromatic (λ dependent).

Pupils



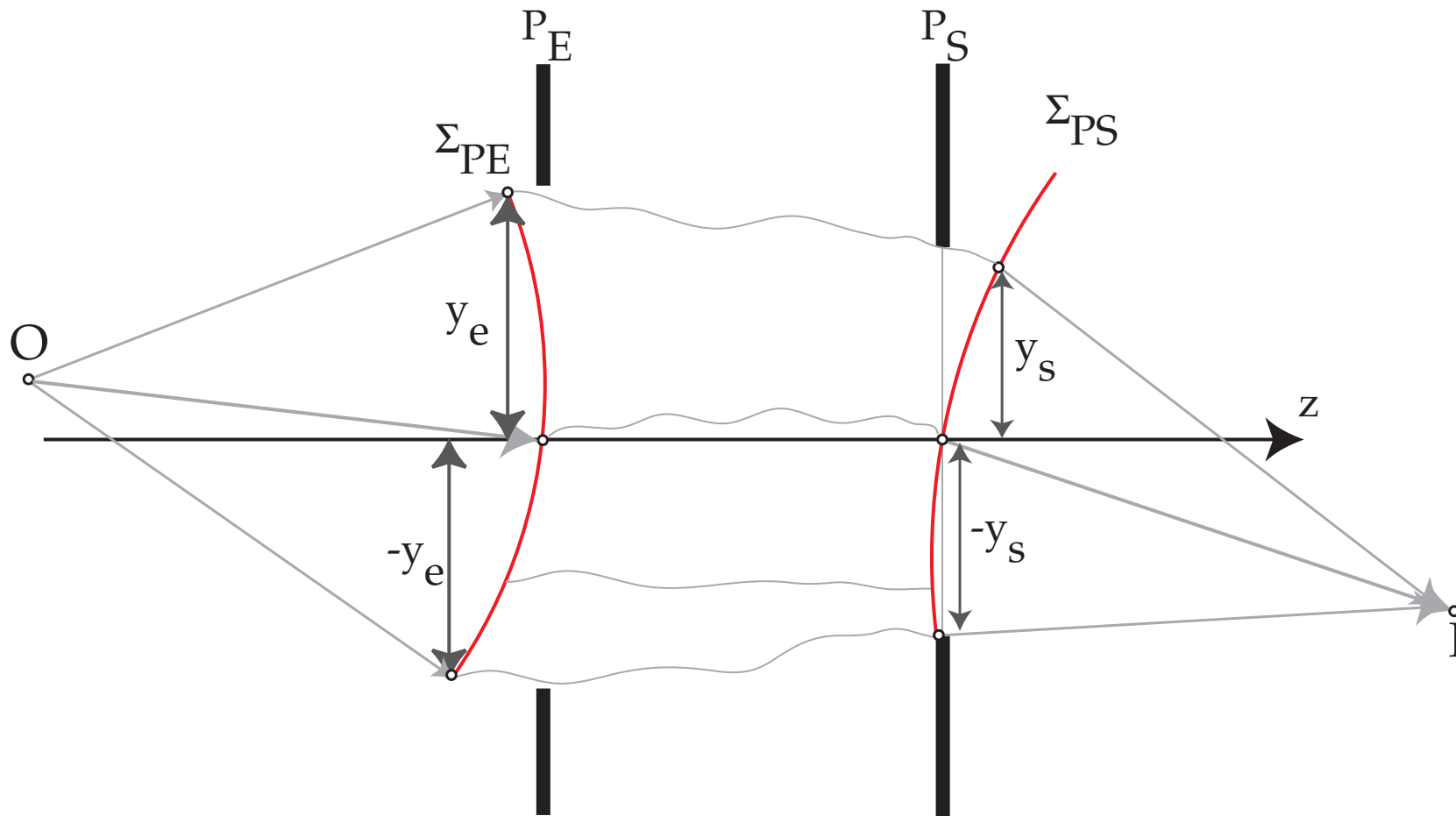
Any optical system can be characterised by an entrance pupil P_e and an exit pupil P_s . The pupils are the image of the opening aperture DO by the entrance and exit optical subsystems SO_e and SO_s . What are P_e and P_s for a thin lens?

In order to evaluate the monochromatic aberrations one must define a function characteristic of the optical system.

This function will depend on:

1. The selected reference planes.
2. The optical path followed by the light ray.

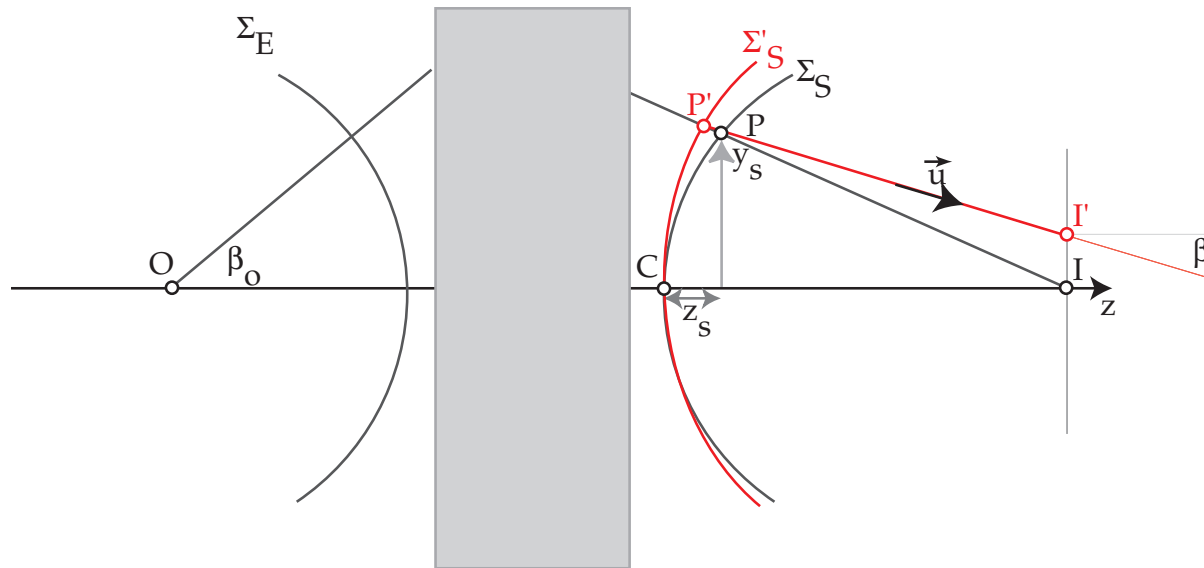
Optical Path Length: OPL



- ▶ **Before** P_E the reference wavefront Σ_{PE} is spherical (point source at O).
- ▶ **After** P_S the reference wavefront Σ_{PS} is spherical (converges towards I).

For a perfect optical system, both the entrance Σ_{PE} and exit Σ_{PS} wavefronts are spherical. The **O**ptical **P**ath **L**ength from O to I is independent of the path.

Optical Path Difference (OPD): aberrations



In the presence of aberrations the wavefront Σ'_S is no more spherical. The **O**ptical **P**ath **D**ifference (distance between the deformed Σ'_S and spherical wavefront Σ_S) introduces a **phase shift** $\delta\phi$. With P' close to $P = (x_s, y_s)$ on reference sphere Σ_S , the OPD at $P' =$ (i.e. OPL from P' to P) is given by (Fermat principle):

$$W(x_s, y_s) = n_i \overline{P'P}$$

n_i refractive index of the medium \longrightarrow phase shift:

$$\delta\phi = e^{2\pi i \frac{W(x_s, y_s)}{\lambda}}$$

Transverse geometric aberrations: $\vec{\epsilon}$

The transverse geometric aberrations are proportional to $\frac{d}{d\theta}$ wavefront aberrations¹³:

$$\epsilon_x = -\frac{f \partial W}{n_i \partial x_s}$$
$$\epsilon_y = -\frac{f \partial W}{n_i \partial y_s}$$

f focal length.

The OPD's introduced by all the aberrations of the imaging system are collected in a function $\chi(\vec{u})$ and the phase shift is¹⁴:

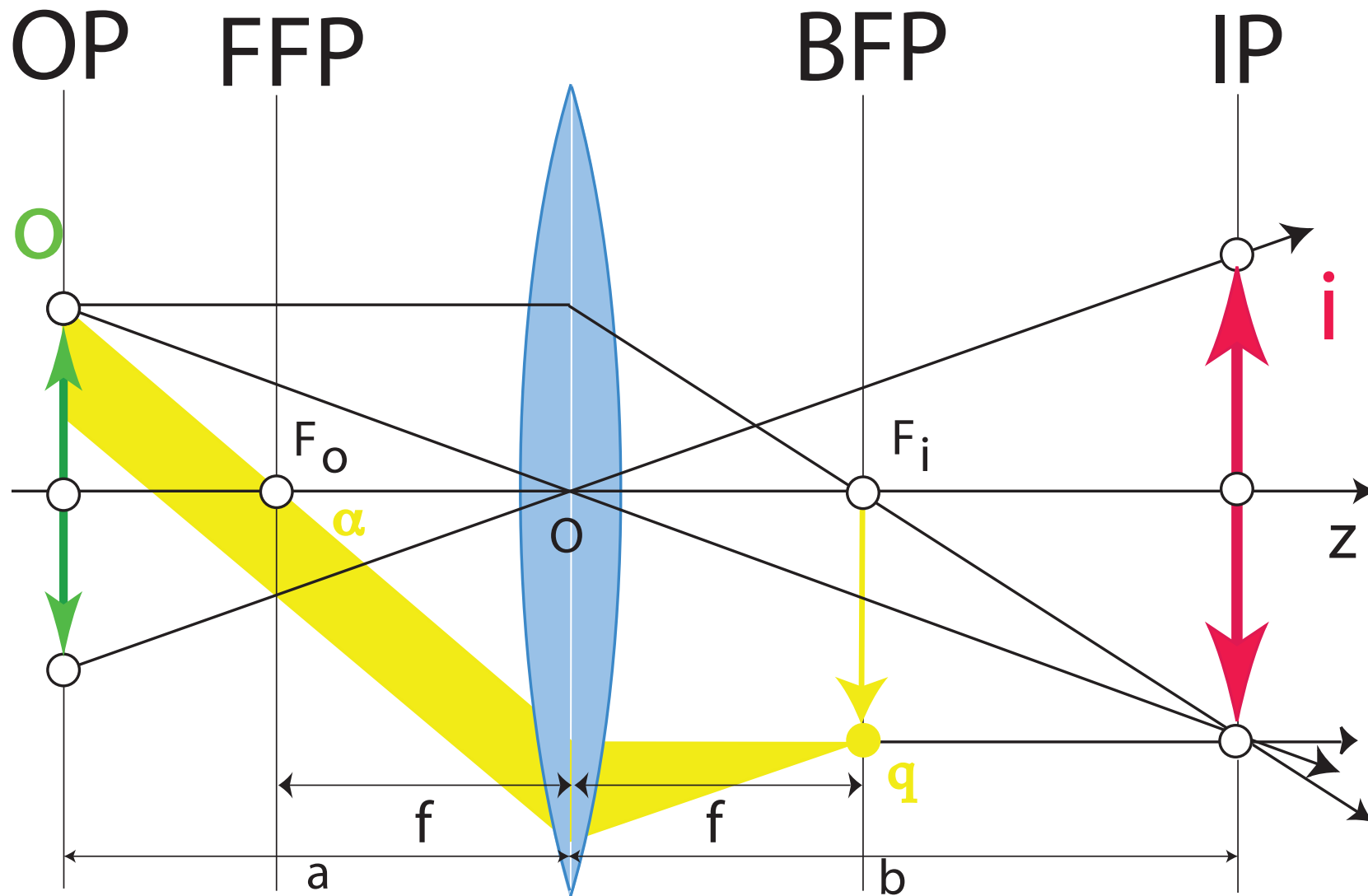
$$\tilde{T}(\vec{u}) = e^{i\chi(\vec{u})}$$

$\tilde{T}(\vec{u})$ has been first employed by Abbe in his description of image formation (1866).

¹³ $P(x_s, y_s)$ on the spherical reference wavefront can be characterised by the radial angle θ .

¹⁴The angle θ corresponds (through Bragg law) to a spatial frequency \vec{u} , i.e. a distance in the back focal plane.

Paraxial optics: principal rays



Principal rays of paraxial optics. Reflection (plane wave) making an angle α , where $\alpha = 2\theta_B$, corresponds to spatial frequency u .

Microscope modelling: Abbe image formation theory

Objective lens is modelled as a thin lens that brings Fraunhofer diffraction pattern at finite distance (i.e. in its **Back Focal Plane**).

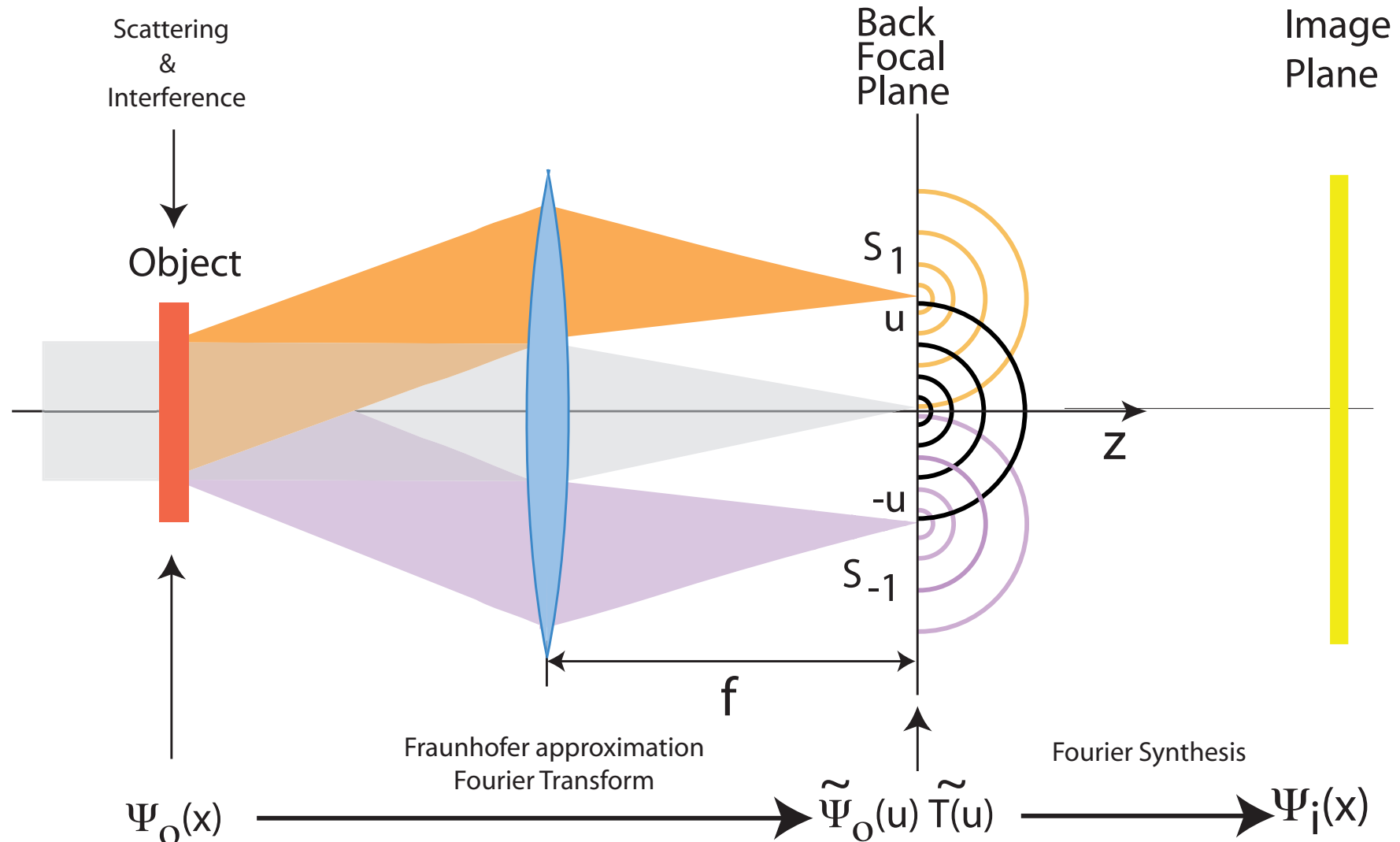


Image forming system has 2 properties (**Abbe theory**):

- ▶ Linear.
- ▶ Space invariant.

Coherence of illumination:

- ▶ Source size (spatial coherence).
- ▶ Energy spread (temporal coherence).

Partial coherence (always the case): $\tilde{T}(q', q)$: transmission cross-coefficients
 \implies is approximated by a transfer function $\tilde{T}(\vec{u})$ and several envelope functions
(attenuation of a range of spatial frequencies)..

Two cases:

→ **TEM** ($\widetilde{T}(\vec{u})$: **T**ransfer **F**unction):

$$\widetilde{\Psi}_i(\vec{u}) = \widetilde{\Psi}_o(\vec{u}) \widetilde{T}(\vec{u})$$

$$\Psi_i(\vec{x}) = \int \widetilde{\Psi}_o(\vec{u}) \widetilde{T}(\vec{u}) e^{2\pi i \vec{u} \cdot \vec{x}} d\vec{u}$$

→ **STEM** ($\widetilde{OTF}(\vec{u}) = \widetilde{T}(\vec{u}) \otimes \widetilde{T}(-\vec{u})$: **O**ptical **T**ransfer **F**unction):

$$I(\vec{x}) = \langle \Psi_i(\vec{x}; t) \Psi_i^*(\vec{x}; t) \rangle$$

$$\Psi_i(\vec{x}; t) = \Psi_o(\vec{x}; t) \otimes T(\vec{x})$$

$$I(\vec{x}) = \langle [\Psi_o(\vec{x}; t) \otimes T(\vec{x})] [\Psi_o^*(\vec{x}; t) \otimes T^*(\vec{x})] \rangle \quad (\otimes \text{ convolution.})$$

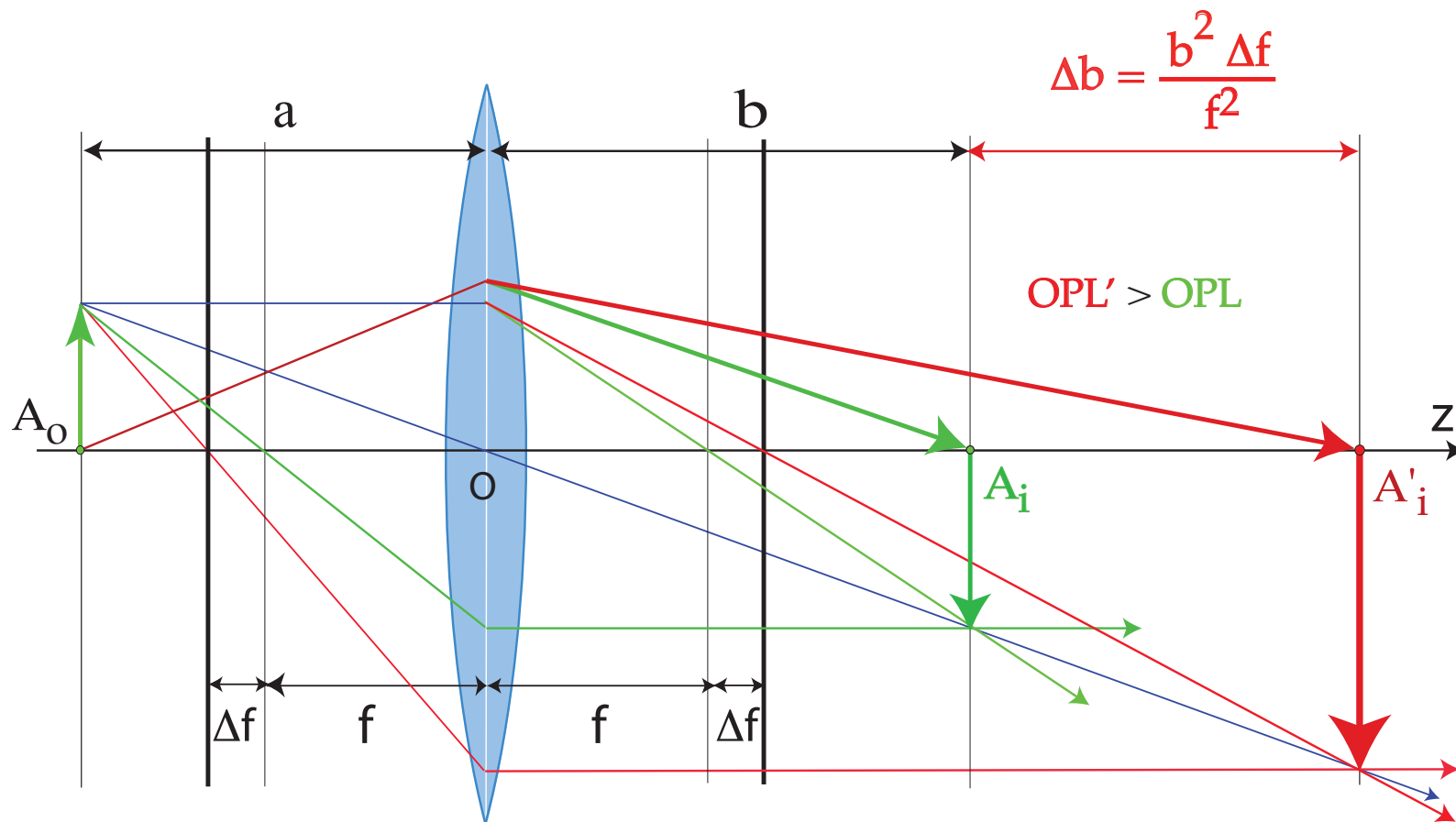
$$I(\vec{x}) = [T(\vec{x}) T^*(\vec{x})] \otimes \langle \Psi_o(\vec{x}; t) \Psi_o^*(\vec{x}; t) \rangle \quad (T(\vec{x}) \text{ is time independent.})$$

$$\langle \Psi_o(\vec{x}; t) \Psi_o^*(\vec{x}; t) \rangle = |\Psi_o(\vec{x})|^2 \quad (\text{complete spatial incoherence})$$

$$I(\vec{x}) = |\Psi_o(\vec{x})|^2 \otimes [T(\vec{x}) T^*(\vec{x})]$$

$$I(\vec{x}) = I_o(\vec{x}) \otimes OTF(\vec{x})$$

Optical Path Length: underfocus



Underfocus weakens the objective lens, i.e. increases f . As a consequence the OPL from A_o to A'_i is larger:

$$e^{2\pi i \frac{\Delta f \lambda (\vec{q} \cdot \vec{q})}{2}}$$

$$T(\vec{q}) = e^{i\chi(\vec{q})} = \cos(\chi(\vec{q})) + i \underbrace{\sin(\chi(\vec{q}))}_{\text{Contrast transfer function}}$$

$$\chi(\vec{q}) = \pi \left[W_{20} \lambda \vec{q} \cdot \vec{q} + W_{40} \frac{\lambda^3 (\vec{q} \cdot \vec{q})^2}{2} + \dots \right]$$

Where:

- ▶ W_{20} : defocus (z)
- ▶ W_{40} : spherical aberration (C_s)

Wave-front aberrations to 6th order (cartesian coordinates)

$$\{z, \pi (u^2 + v^2) \lambda\} \text{ (defocus)}$$

$$\{W(1, 1), 2\pi(u \cos(\phi(1, 1)) + v \sin(\phi(1, 1)))\}$$

$$\{W(2, 2), \pi\lambda((u - v)(u + v) \cos(2\phi(2, 2)) + 2uv \sin(2\phi(2, 2)))\}$$

$$\{W(3, 1), \frac{2}{3}\pi (u^2 + v^2) \lambda^2(u \cos(\phi(3, 1)) + v \sin(\phi(3, 1)))\}$$

$$\{W(3, 3), \frac{2}{3}\pi\lambda^2 (u (u^2 - 3v^2) \cos(3\phi(3, 3)) - v (v^2 - 3u^2) \sin(3\phi(3, 3)))\}$$

$$\left\{ W(4, 0), \frac{1}{2}\pi (u^2 + v^2)^2 \lambda^3 \right\} \text{ (3rd order spherical aberration or } C_3)$$

$$\{W(4, 2), \frac{1}{2}\pi (u^2 + v^2) \lambda^3((u - v)(u + v) \cos(2\phi(4, 2)) + 2uv \sin(2\phi(4, 2)))\}$$

$$\{W(4, 4), \frac{1}{2}\pi\lambda^3 ((u^4 - 6v^2u^2 + v^4) \cos(4\phi(4, 4)) + 4u(u - v)v(u + v) \sin(4\phi(4, 4)))\}$$

$$\left\{ W(5, 1), \frac{2}{5}\pi (u^2 + v^2)^2 \lambda^4(u \cos(\phi(5, 1)) + v \sin(\phi(5, 1))) \right\}$$

$$\{W(5, 3), \frac{2}{5}\pi (u^2 + v^2) \lambda^4 (u (u^2 - 3v^2) \cos(3\phi(5, 3)) - v (v^2 - 3u^2) \sin(3\phi(5, 3)))\}$$

$$\{W(5, 5), \frac{2}{5}\pi\lambda^4 (u (u^4 - 10v^2u^2 + 5v^4) \cos(5\phi(5, 5)) + v (5u^4 - 10v^2u^2 + v^4) \sin(5\phi(5, 5)))\}$$

$$\left\{ W(6, 0), \frac{1}{3}\pi (u^2 + v^2)^3 \lambda^5 \right\} \text{ (5th order spherical aberration or } C_5)$$

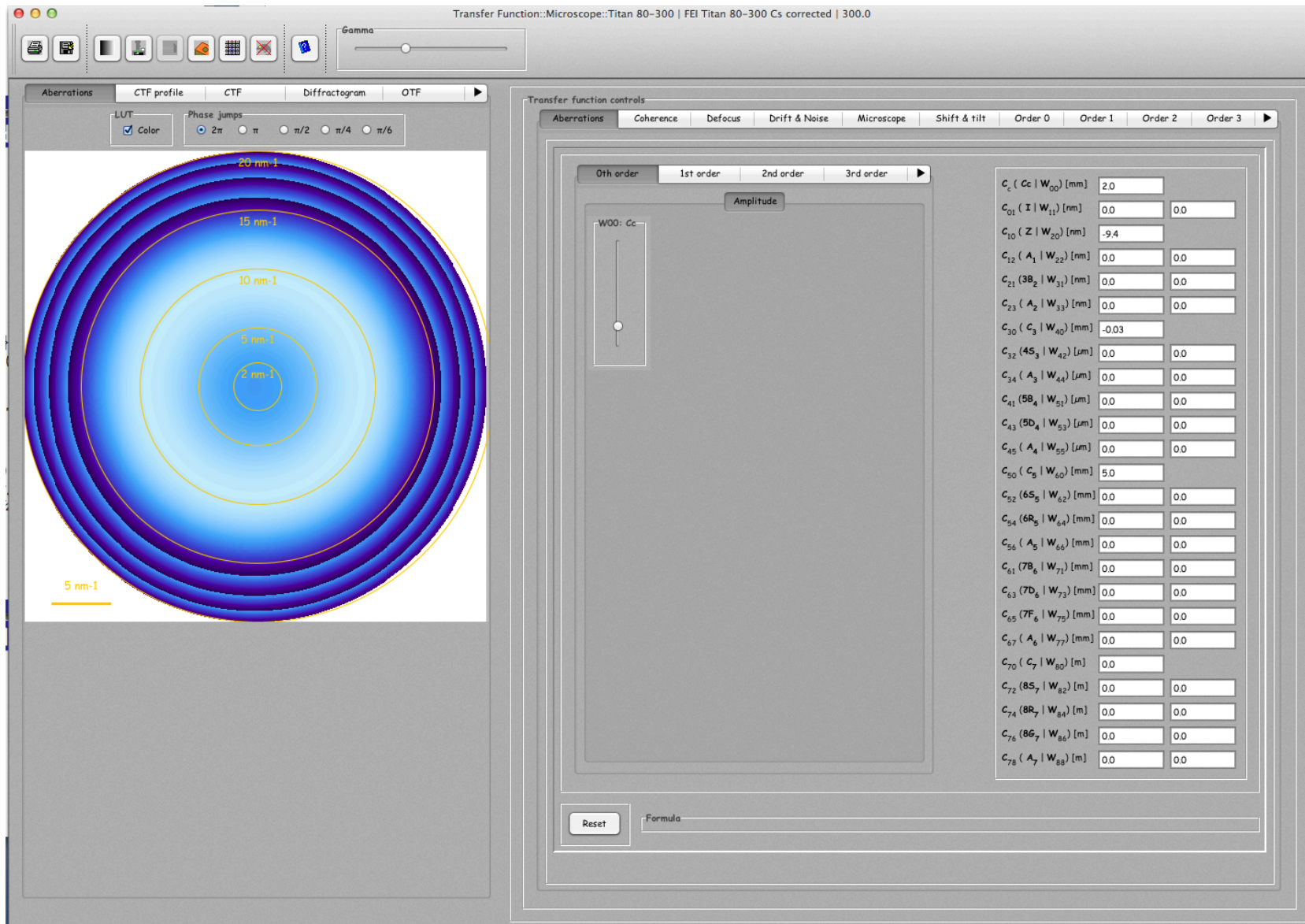
$$\{W(6, 2), \frac{1}{3}\pi (u^2 + v^2)^2 \lambda^5((u - v)(u + v) \cos(2\phi(6, 2)) + 2uv \sin(2\phi(6, 2)))\}$$

$$\{W(6, 4), \frac{1}{3}\pi\lambda^5 ((u^6 - 5v^2u^4 - 5v^4u^2 + v^6) \cos(4\phi(6, 4)) + 4uv (u^4 - v^4) \sin(4\phi(6, 4)))\}$$

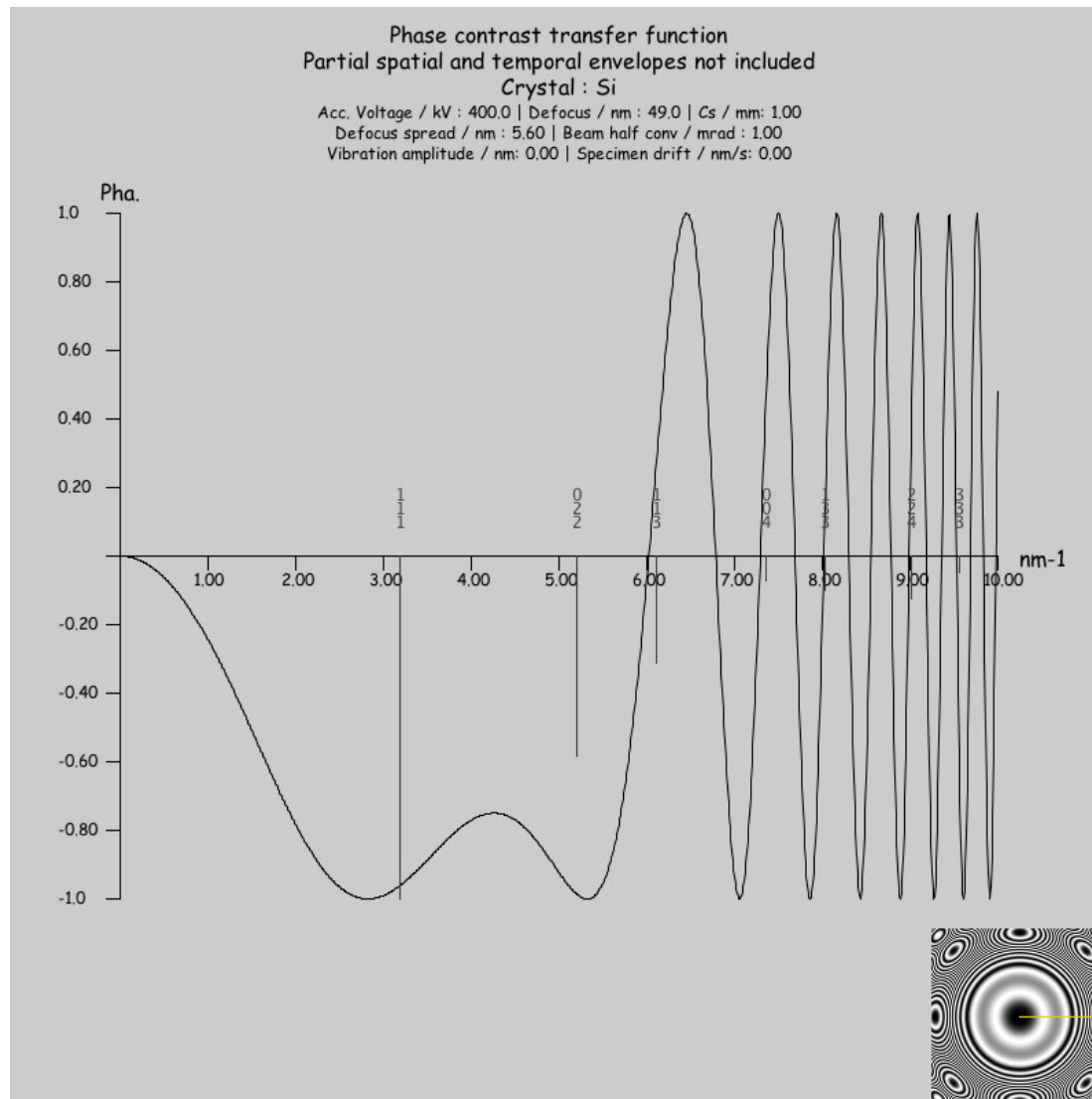
$$\{W(6, 6), \frac{1}{3}\pi\lambda^5 ((u^6 - 15v^2u^4 + 15v^4u^2 - v^6) \cos(6\phi(6, 6)) + 2uv (3u^4 - 10v^2u^2 + 3v^4) \sin(6\phi(6, 6)))\}$$

jems describes wave-front aberrations to order 8.

Wave-front aberrations to order 8



Contrast transfer function: $\sin(\chi(\vec{q}))$



The transfer function of the objective lens in the absence of lens current and accelerating voltage fluctuations (Scherzer defocus). The (111) and (022) reflections of Si are phase shifted by $-\frac{\pi}{2} \rightarrow$ black atomic columns.

In the **W**eak **P**hase **O**bject **A**pproximation under **optimum transfer conditions** the image intensity $I(\vec{x})$ is:

- ▶ positive C_s (black atomic columns)

$$I(\vec{x}) \sim 1 - 2\sigma V_p(\vec{x})$$

- ▶ negative C_s (white atomic columns)

$$I(\vec{x}) \sim \sigma V_p(\vec{x})$$

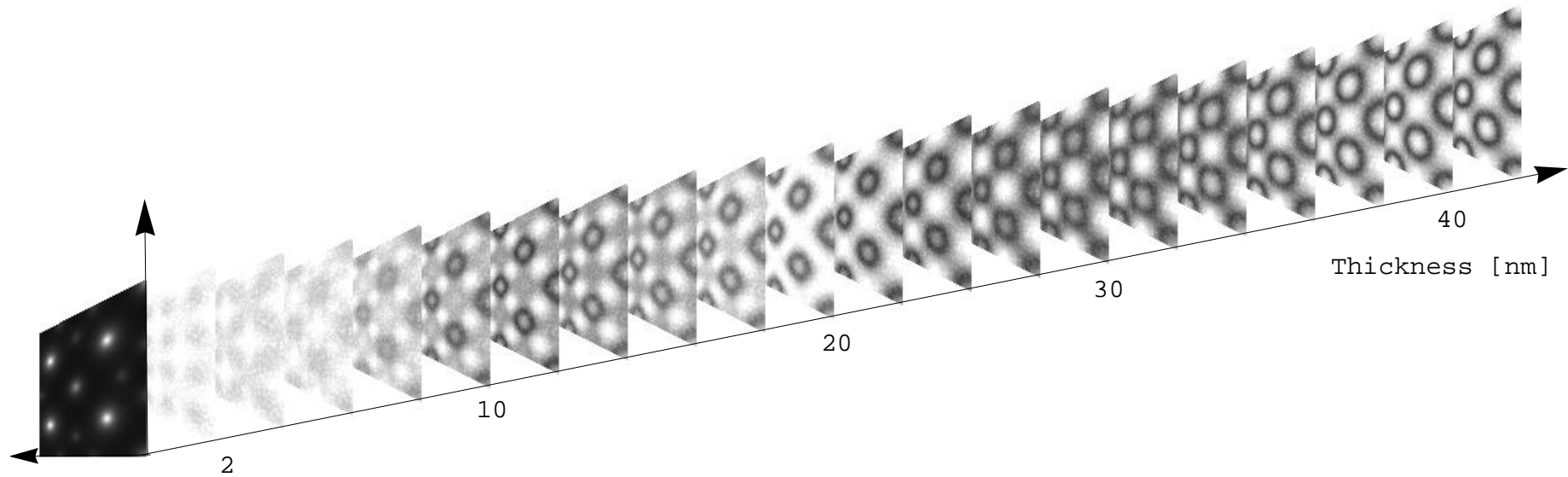
Where:

$V_p(\vec{x})$: projected potential

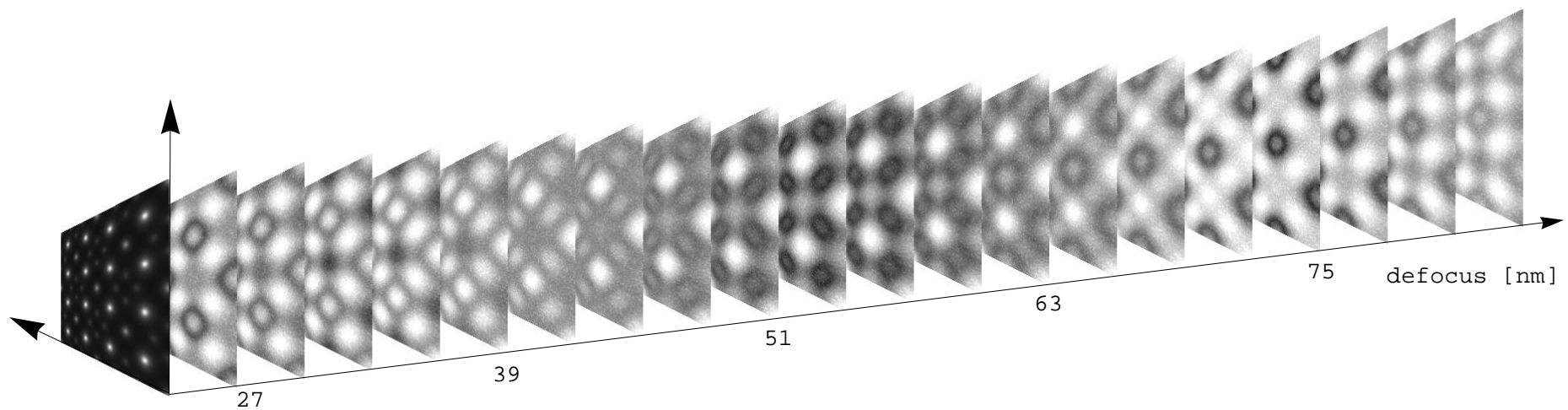
σ : electron matter interaction constant

HRTEM image depends on specimen thickness and object defocus

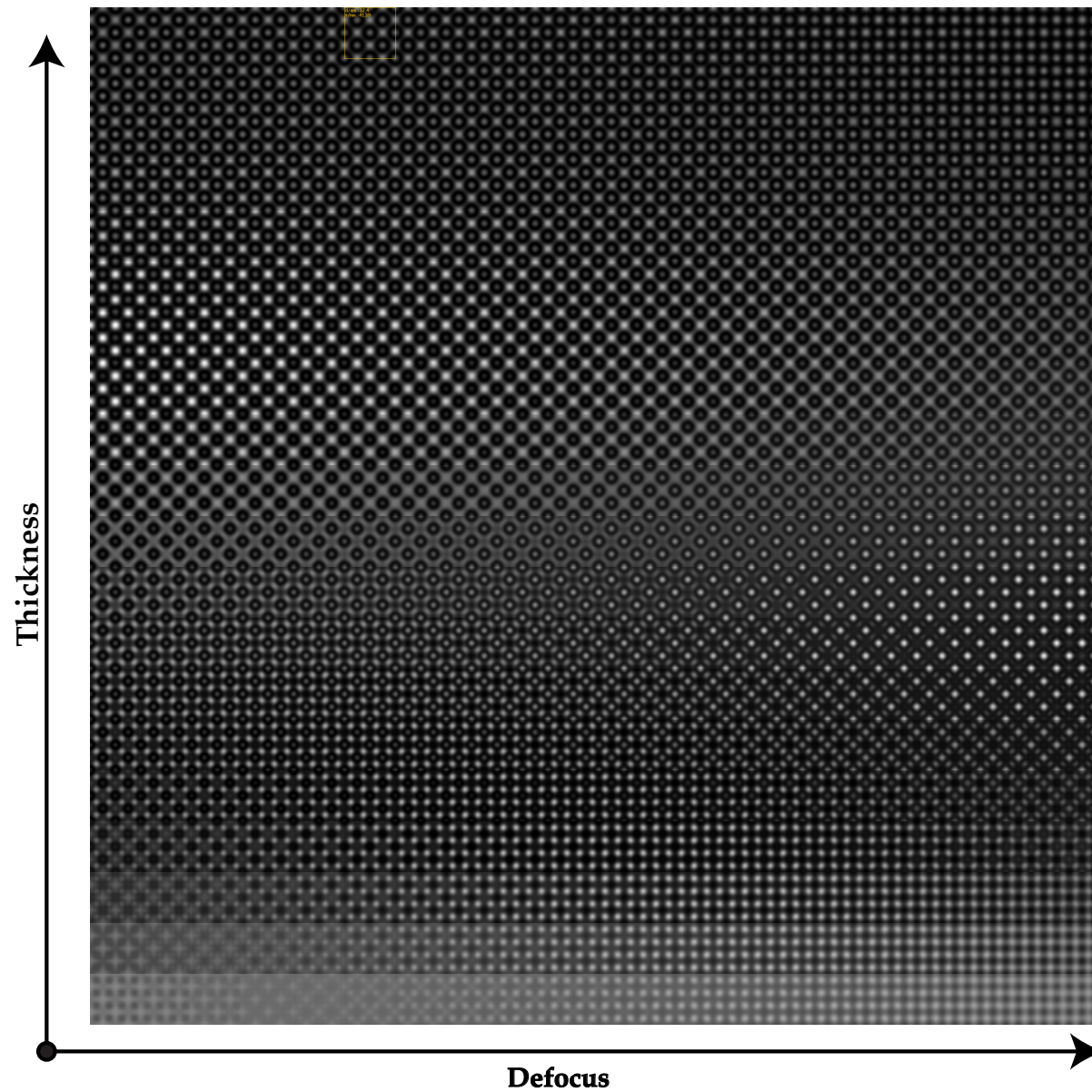
Thickness series



Defocus series



Si [001] images map: contrast dependence of defocus & thickness



HREM map does not include the Modulation Transfer Function (MTF) of the detector.

Details¹⁵

How to reach a **perfect match** between experimental and simulated images?

1. Models (crystal, elastic, inelastic scattering, dynamical theory, imaging).
2. Image acquisition.
3. Environment.
4. ...

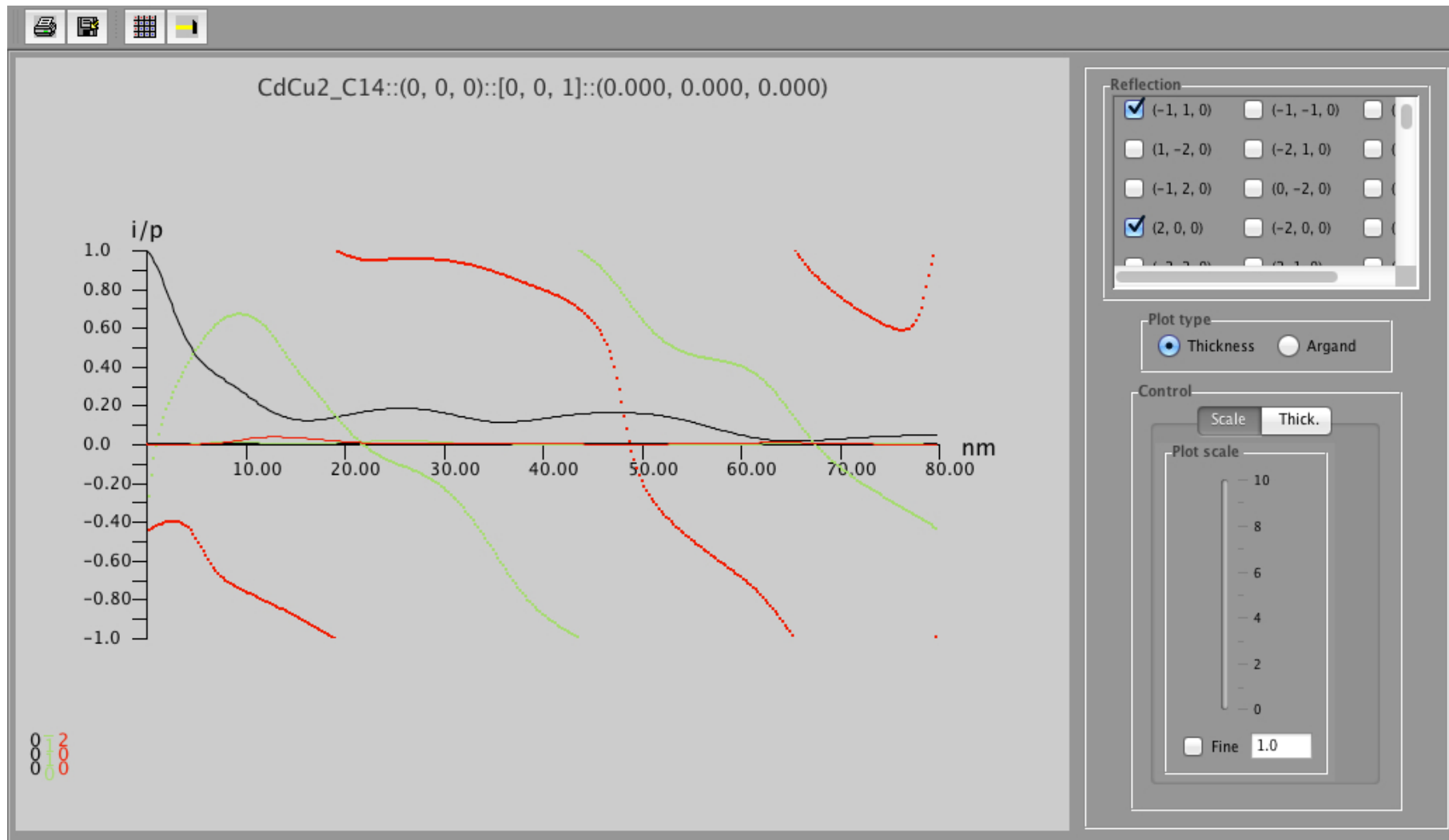
How to define a perfect match?

¹⁵The devil is in the details!

- ▶ Object
 - ▶ → Atomic scattering amplitude below 50 kV?
 - ▶ → Potential by DFT calculation?
 - ▶ ...
- ▶ HRTEM → Phase of diffracted beams evolves with specimen thickness.
- ▶ HRTEM → MTF of image acquisition system (Stobbs factor?).
- ▶ HRTEM / HRSTEM → Electron channeling depends on atomic column content.
- ▶ HRTEM / HRSTEM → Aberrations of optical system.
- ▶ HRTEM → Inelastic scattering (J.M. Cowley, E.J. Kirkland, D. van Dyck, A. Rosenaurer, K. Ishizuka, Z.L. Wang, H. Rose, H. Mueller, L. Allen, ...).
- ▶ HRTEM / HRSTEM → Drift, vibration, Johnson-Nyquist noise¹⁶, ...
- ▶ ...

¹⁶S. Uhlemann, H. Mueller, P. Hartel, J. Zach & M. Haider, Phys. Rev. Lett. **111** (2013) 046101.

HRTEM problem: amplitude and phase of diffracted beams



Note that phase of diffracted beam is $\frac{\pi}{2}$ out-of-phase with respect to transmitted beam.

HRTEM problem: CCD MTF (Gatan MSC 1K x 1K, 24 μm)

To make quantitative comparison with experimental HRTEM images the MTF of the detector must be introduced in the simulation.

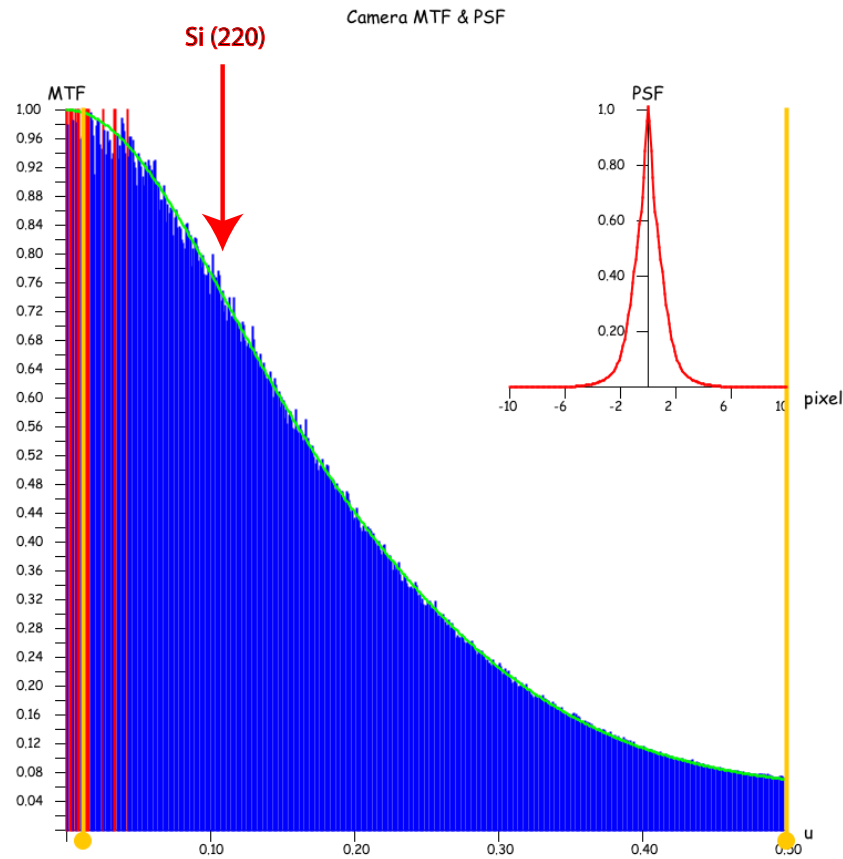


Figure: At high magnification Si (220) planes imaged with high contrast.

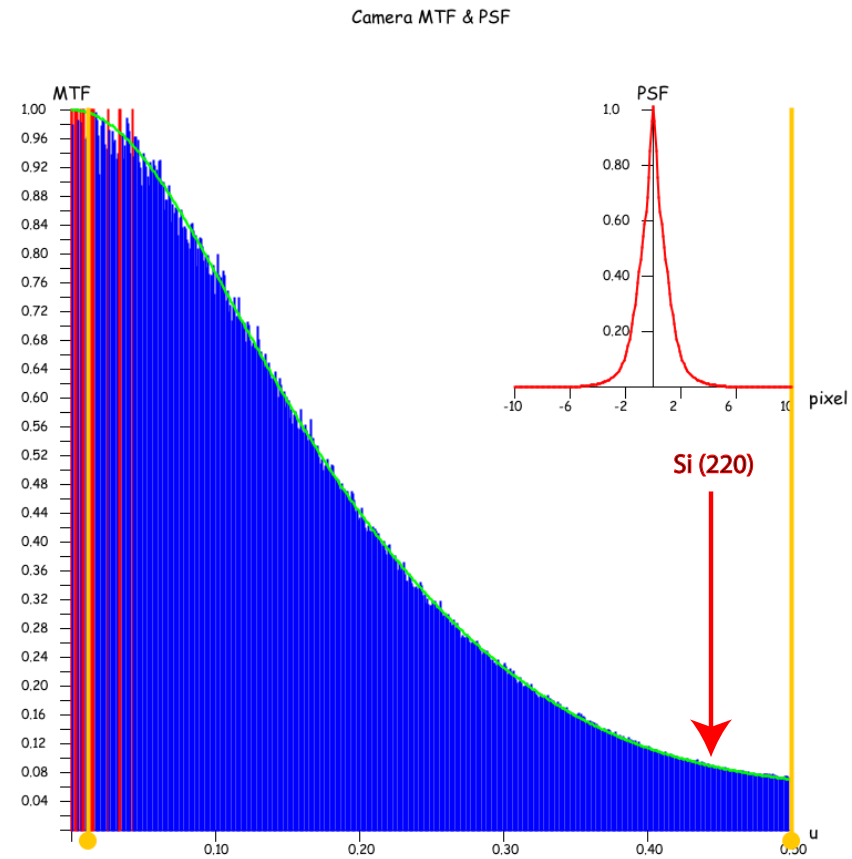


Figure: At low magnification Si (220) planes imaged with low contrast.

For quantitative comparison always use highest possible magnification (or include CCD MTF in simulations)!

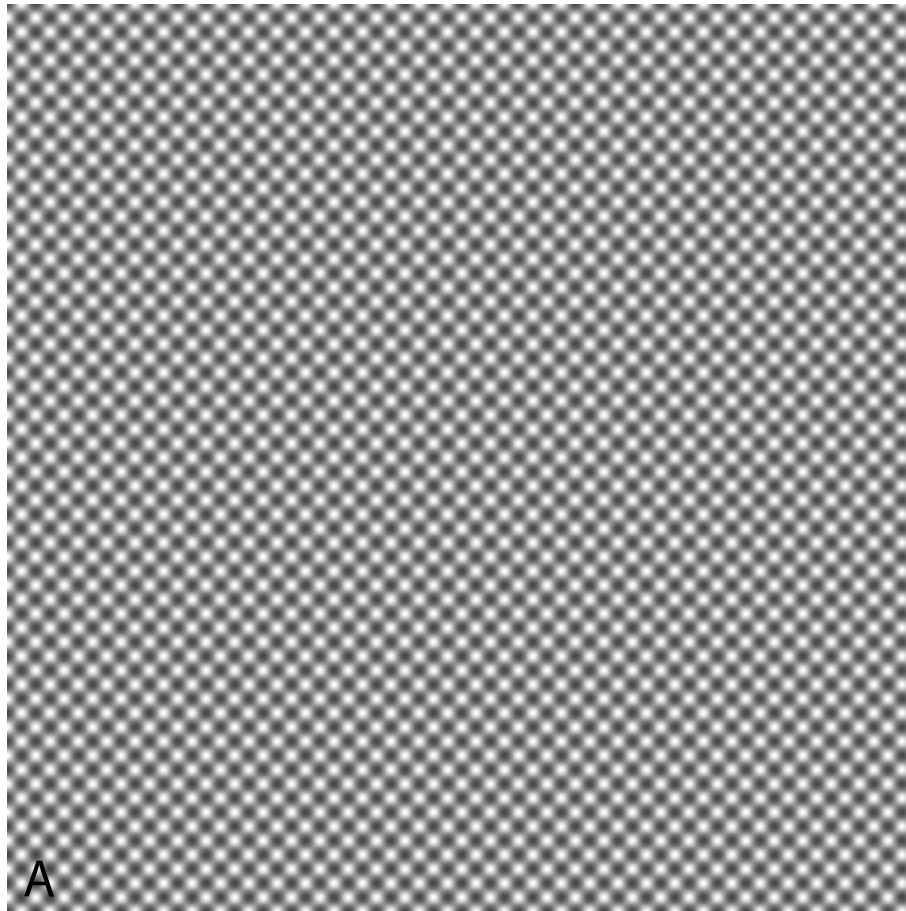


Figure: A: Si [001] simulation.

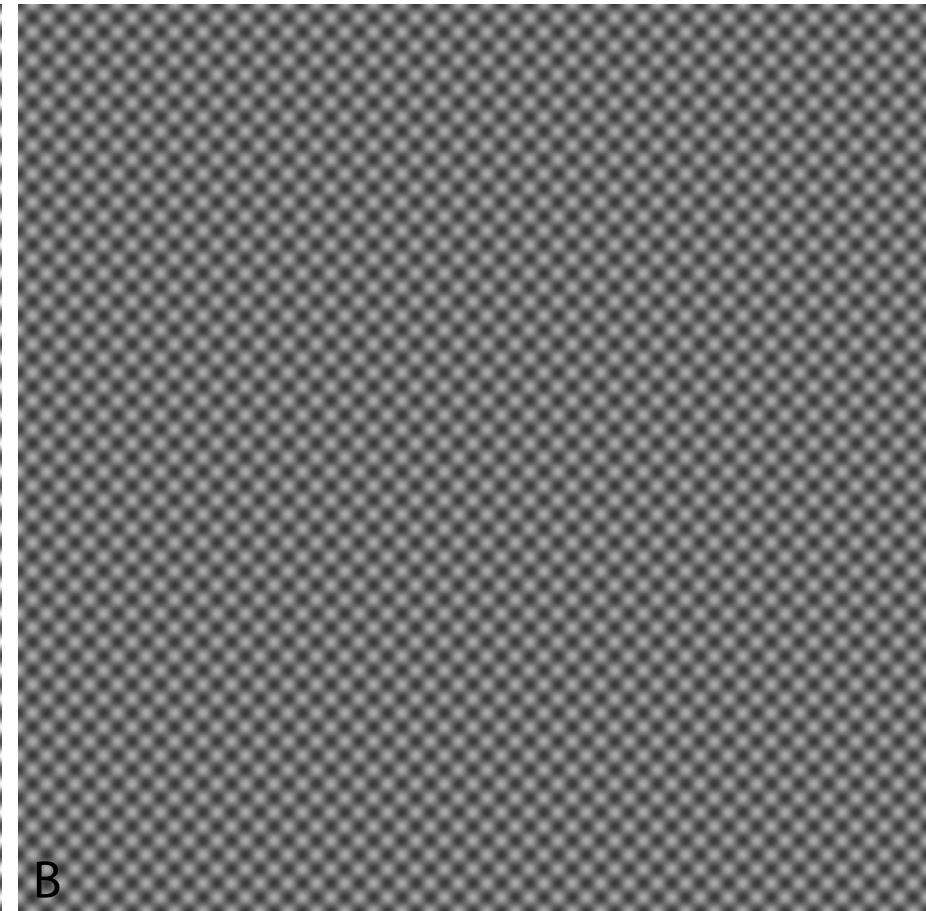


Figure: B: Si [001], simulation + CCD MTF.

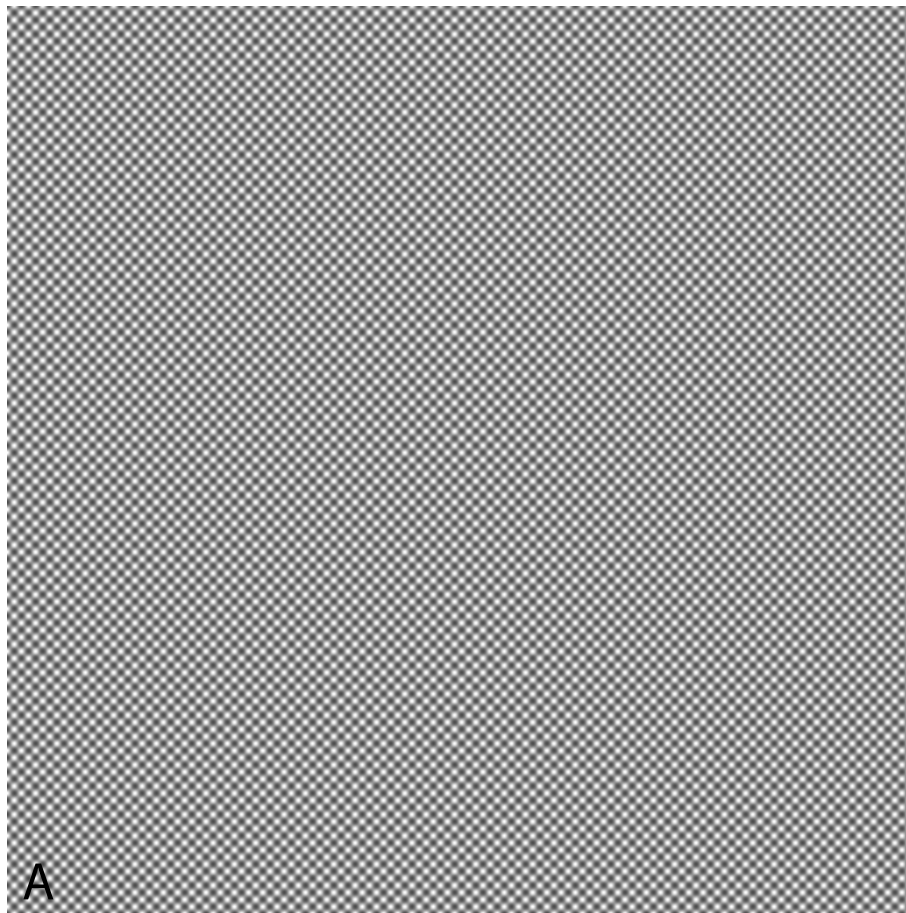


Figure: A: Si [001] simulation.

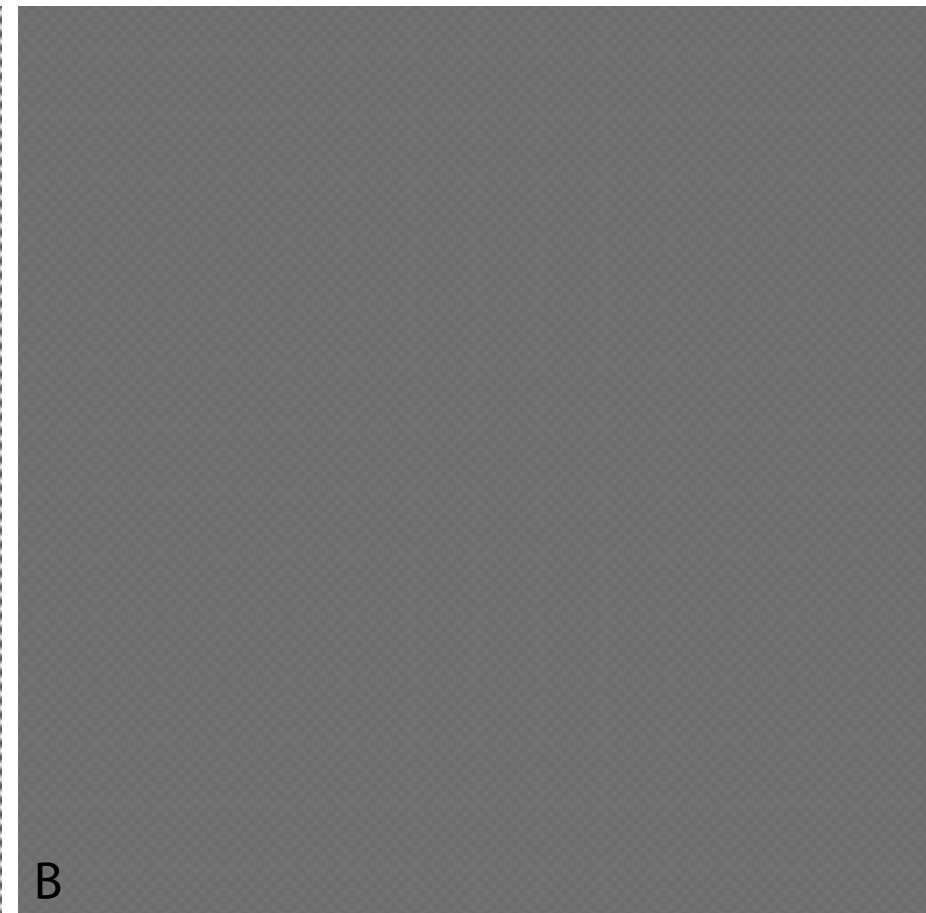


Figure: B: Si [001], simulation + CCD MTF.

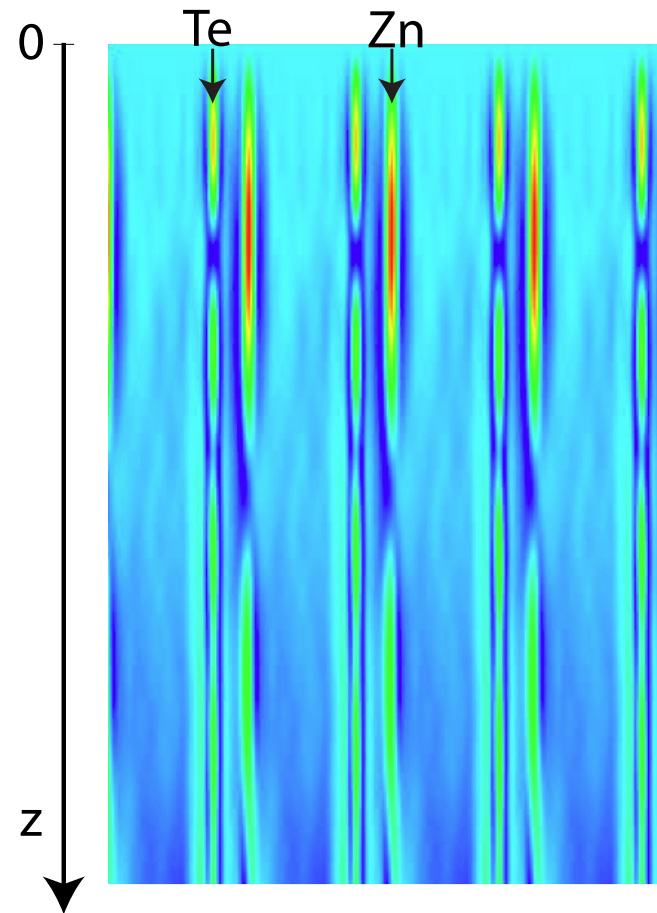
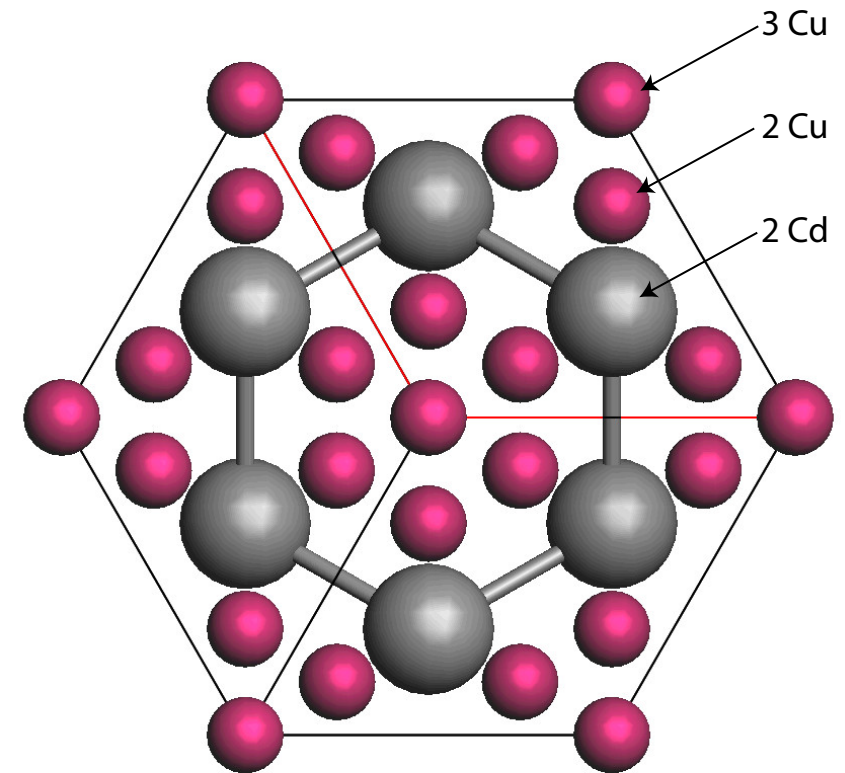
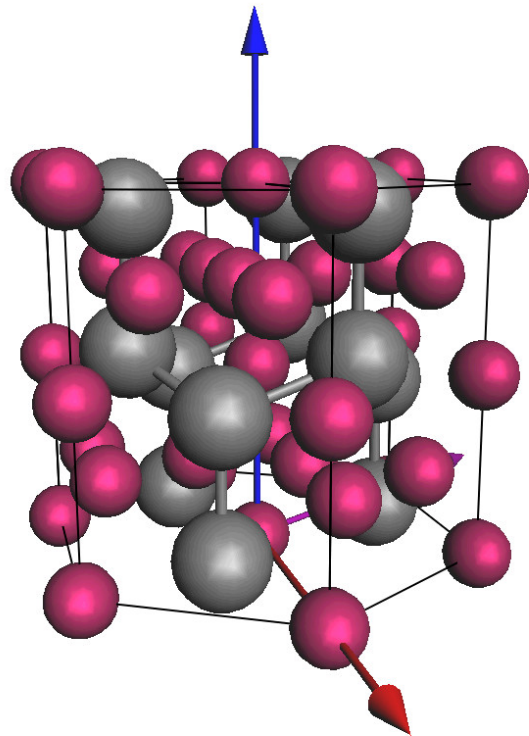


Figure: ZnTe [110] wave function intensity.

Channeling explains several features of HRTEM and STEM images (i.e. appearance / disappearance of contrast of impurities).

Does C_s and C_c correction solves all imaging problems?

Example: CdCu_2 , visibility of the 3 Cu atomic columns.

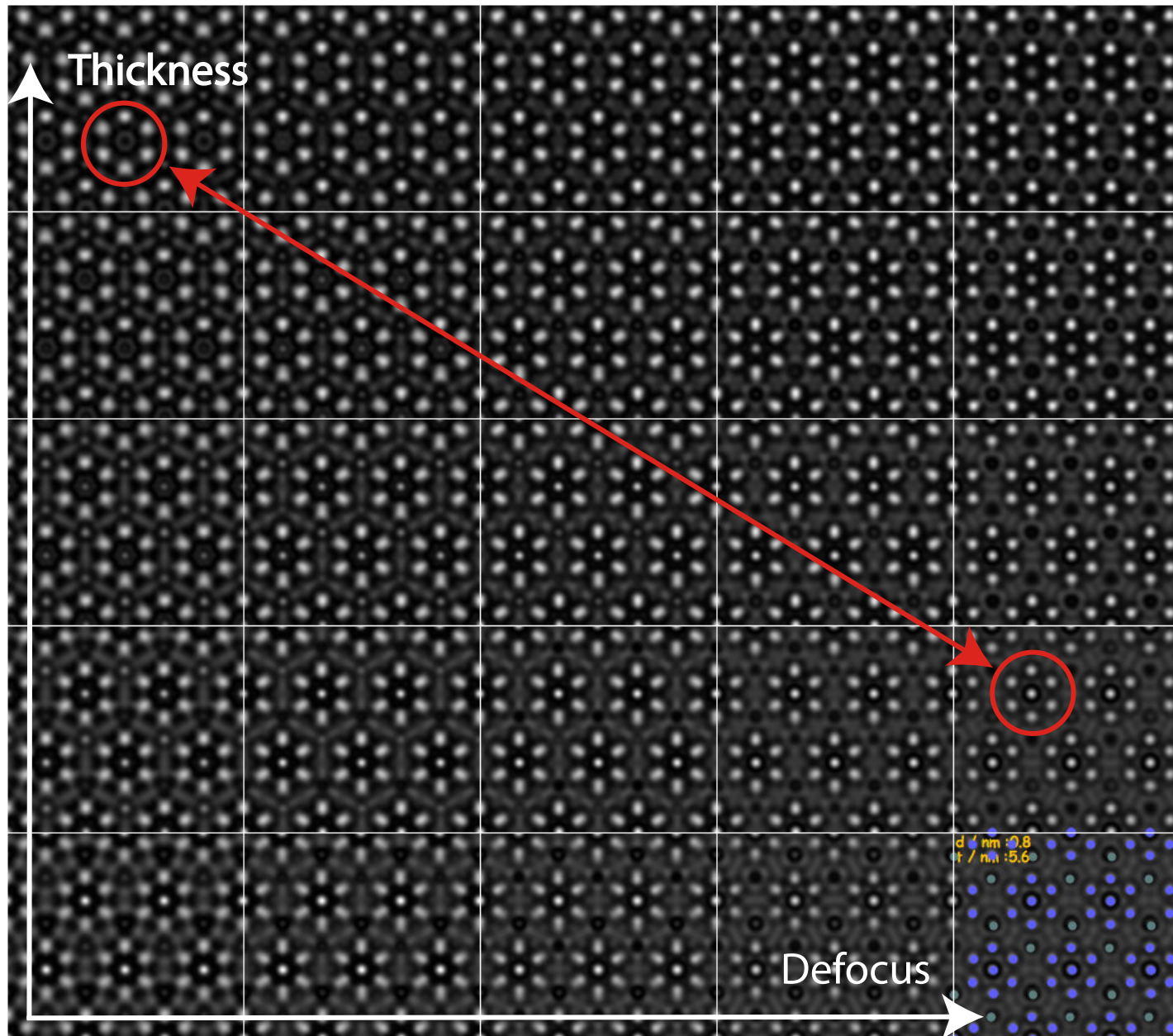


HRTEM image simulation conditions

Acc. [kV]	C_s [mm]	C_5 [mm]	C_c [mm]	ΔE [eV]	Z [nm]	Δz [nm]
300	-0.008	30	0.5	0.6	-4.9	1
300	-0.008	30	0.1	0.2	-2.0	1

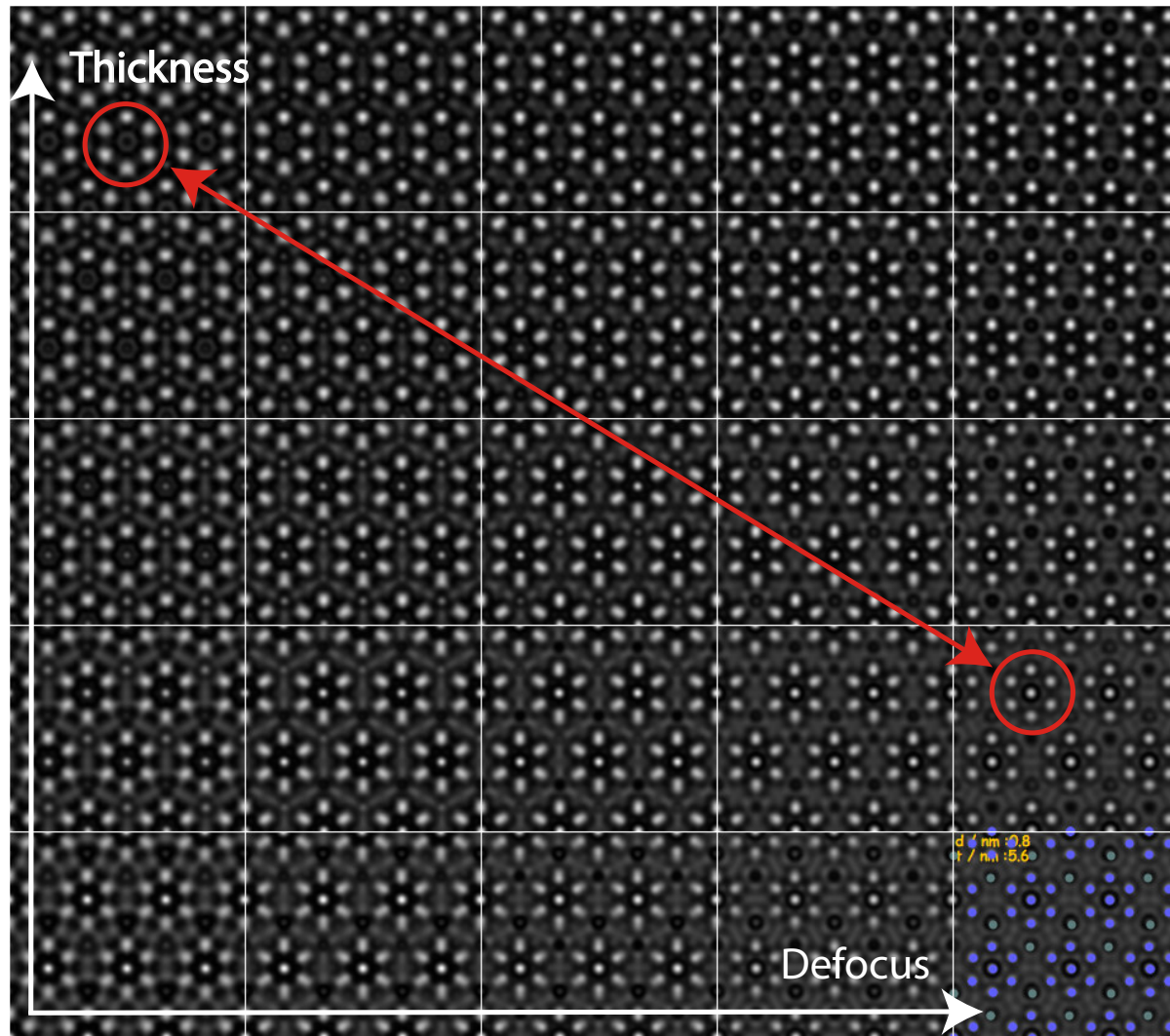
Dynamical scattering effects are not affected by C_s and/or C_c corrected TEM!

$CdCu_2[001]$: imaging parameters set 1



Visibility of 3 Cu atomic columns depends on specimen thickness and defocus.

$CdCu_2[001]$: imaging parameters set 2



Improving C_c and ΔE does not affect the visibility of 3 the Cu atomic columns. It depends on specimen thickness (and defocus indeed). Visibility of the 3 Cu atomic columns is **always** affected by dynamical scattering. Only extremely thin specimen (≤ 10 nm) will allow **faithful** imaging of crystal projected potential.

High Angle Annular Dark Field (HAADF): inelastically scattered electrons.

When simulation is necessary how to simulate images?

Numerous approximations:

- ▶ Simple projected + convolution with probe intensity: no channeling effect (**Weak Object Approximation**).
- ▶ Multislice calculation: channeling + inelastic scattering (absorption potential) + convolution with probe intensity.
- ▶ Frozen lattice (phonon) approximation: atoms of super-cell displaced out of equilibrium position, probe scanned on imaged area, intensity collected by annular detector.
- ▶ Pennycook, Nellist, Ishizuka, Shiojiri, Allen, Wang, Rosenauer, van Dyck, ...

Except the first 2 methods, simulation time expensive (**luxury?**). Approximations (**necessity**) may suffice...

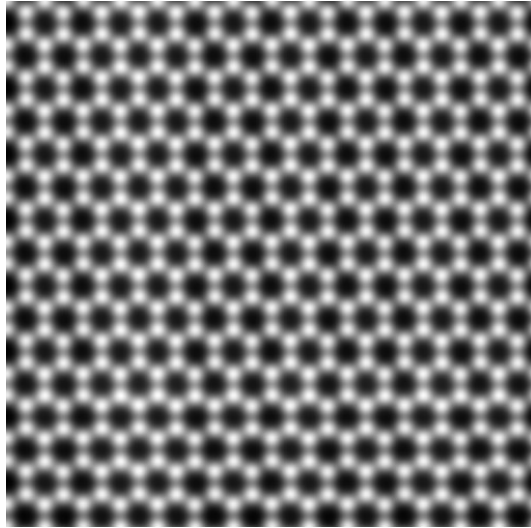


Figure: Proj. pot. approx.



Figure: Channeling calculation.

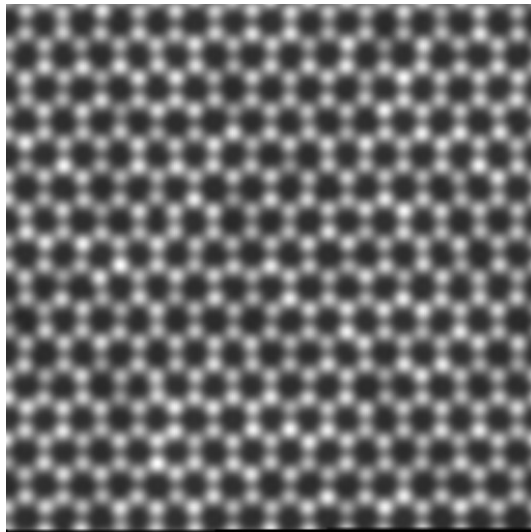


Figure: Frozen lattice 5 conf.

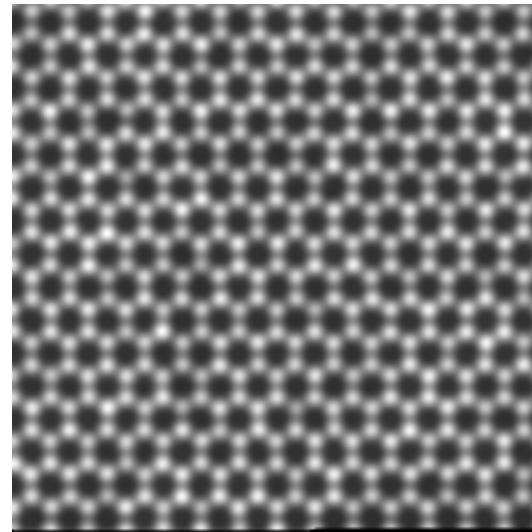


Figure: Frozen lattice 10 conf.

HRSTEM - HRTEM comparison: graphene with add atoms

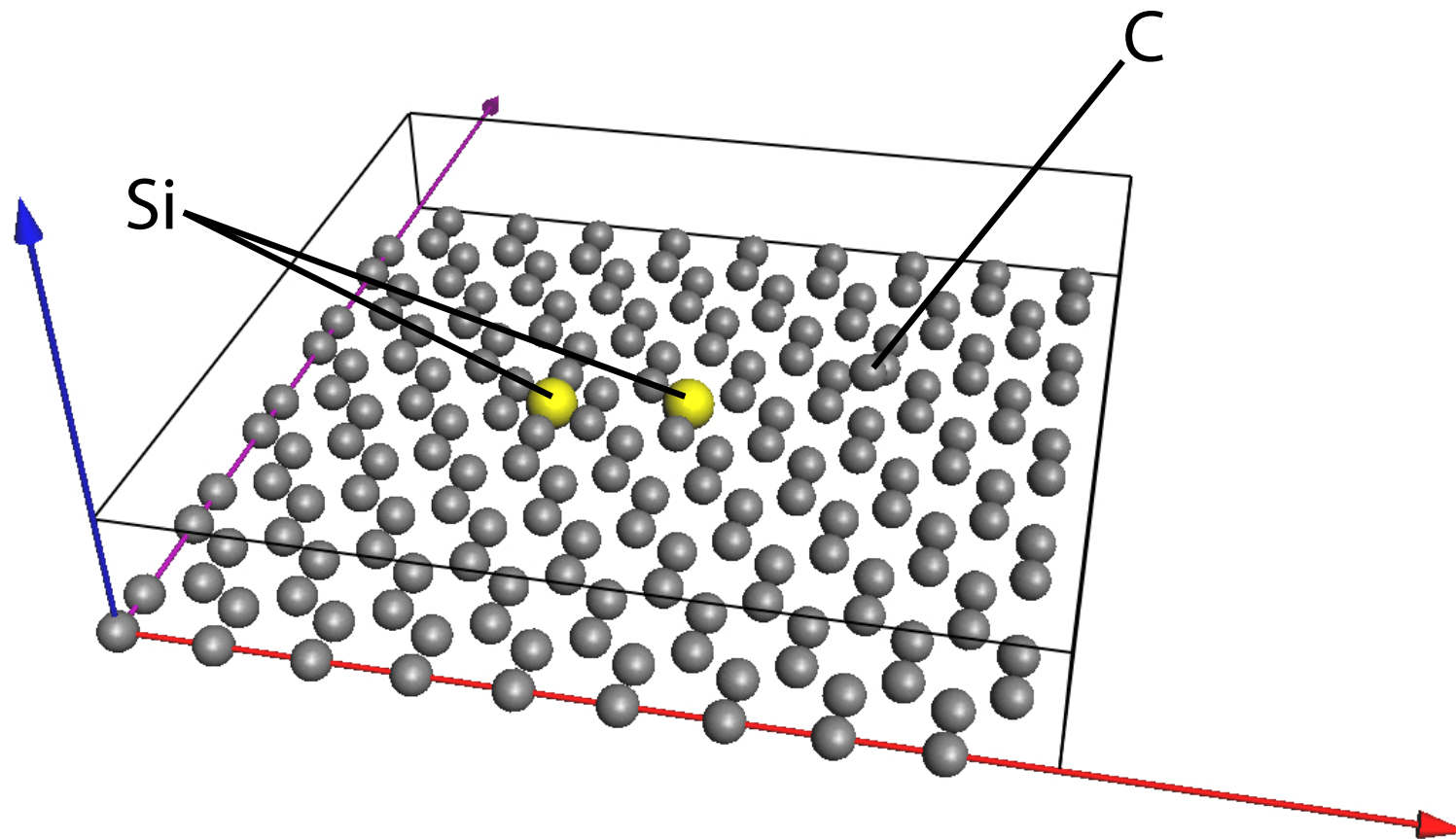


Figure: Graphene with Si in 6 C ring, Si substitutional and 2 C column.

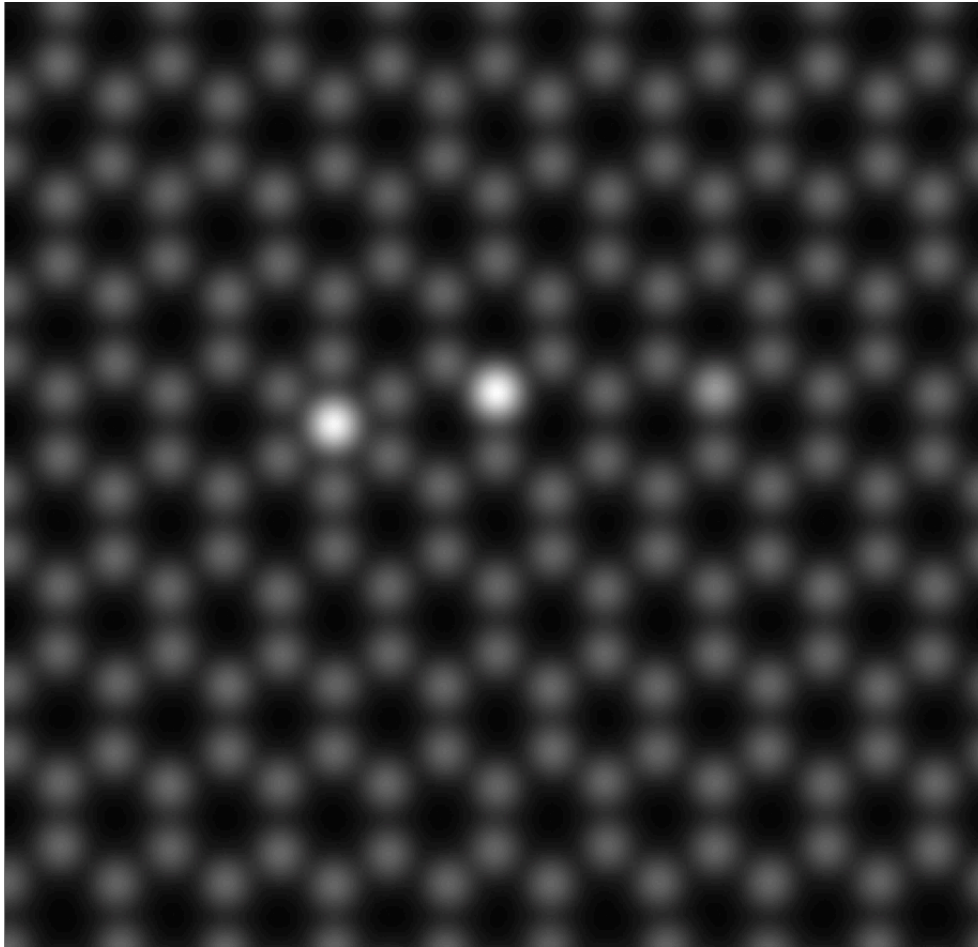


Figure: Frozen lattice (~ 400 s).



Figure: Channeling (~ 2 s).

One Si shows more contrast than 2 C atoms ($i \sim Z^2$) : 14^2
compared to $\sim 2 \times 6^2$.

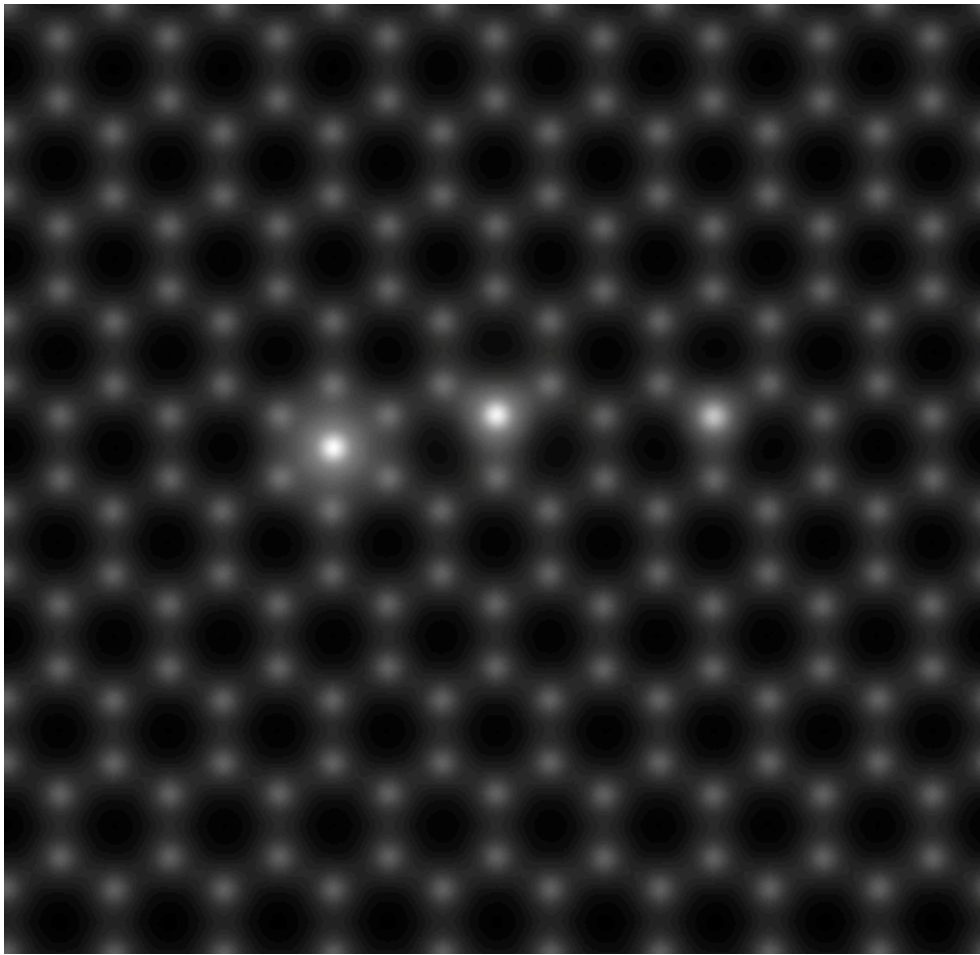


Figure: Weak phase object app., $C_c = 0.5\text{mm}$

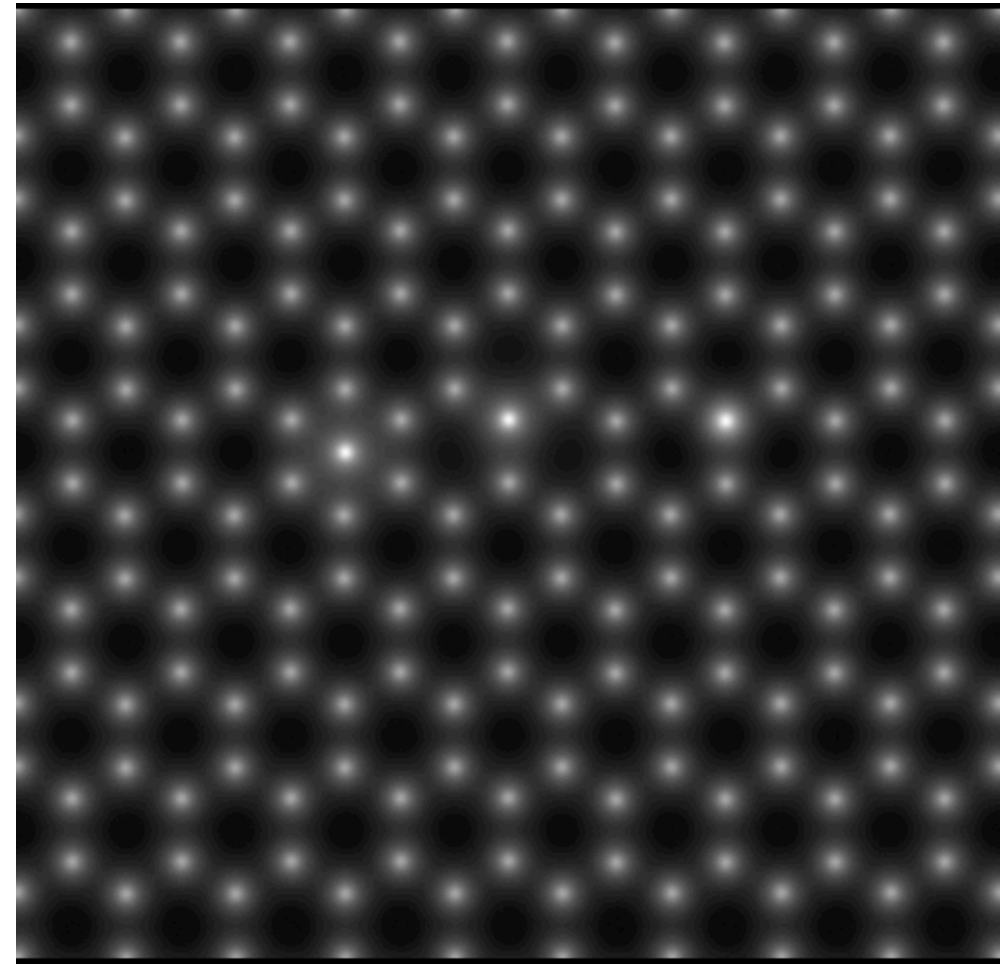


Figure: Multislice, $C_s = -0.033\text{mm}$, $C_c = 0$, no thermal magnetic noise.

HRTEM does not display the strong contrast difference between one Si and two C as given by HAADF.

Image simulation still necessary for quantitative work¹⁷.

Exit wave function recovery possible using:

- ▶ Focal series reconstruction.
- ▶ Transport of intensity equation.

Crystal structure determination not (yet) possible, inverse dynamical scattering cannot be solved in general.

¹⁷K. W. Urban, Science **321** (2008) 506.

Thanks for your attention!

Reaching 0.05 nm resolution sets very strong conditions on aberrations correction.

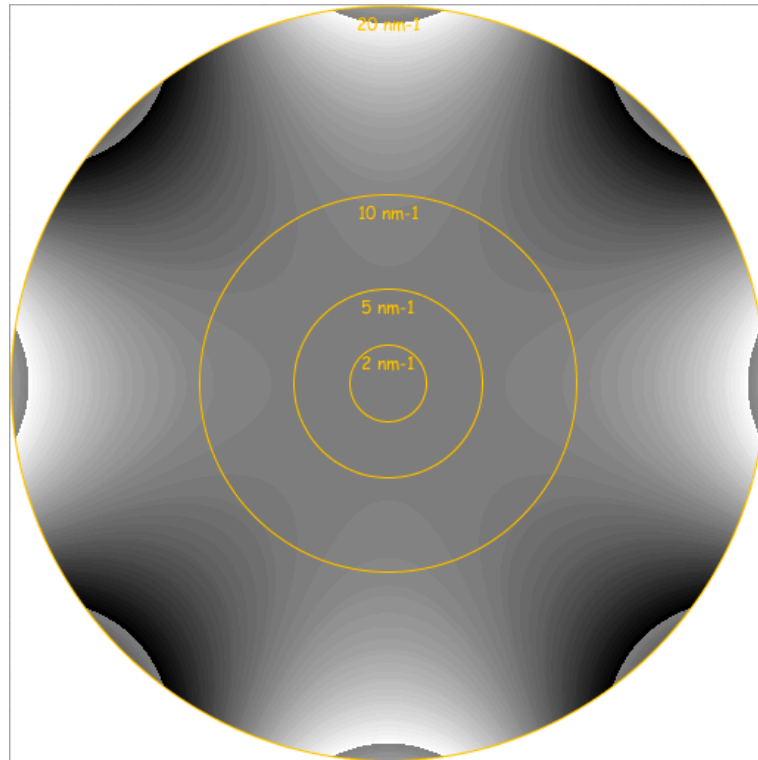


Figure: Aberration figure of $C_{34}(0.5\mu\text{m})$, phase jump at $\frac{\pi}{4}$.

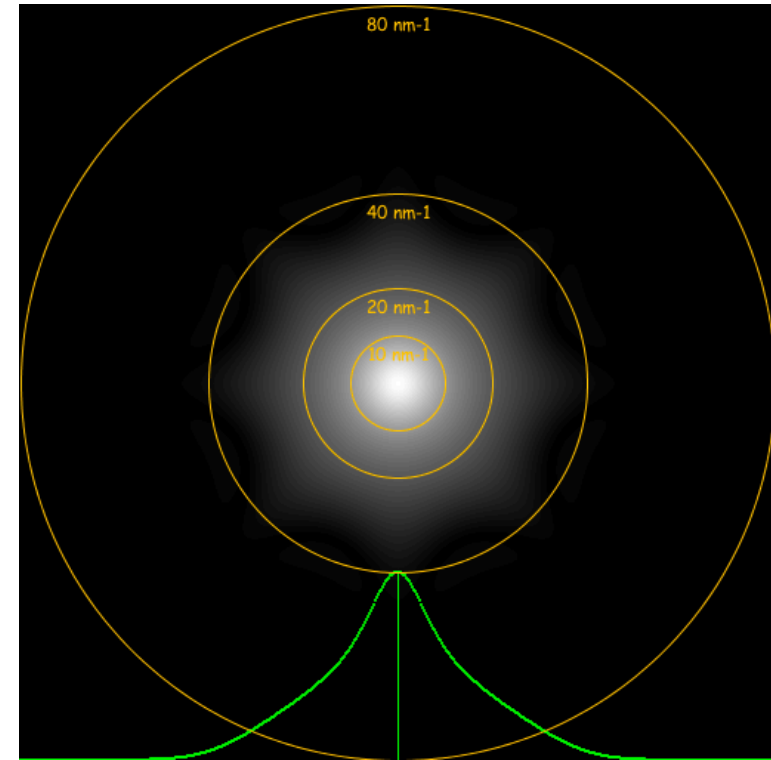


Figure: Optical Transfer Function.

Note that Optical Transfer Function (HRSTEM) transfers higher spatial frequencies than Ccoherent Transfer Function (HRTEM).

HAADF: graphene

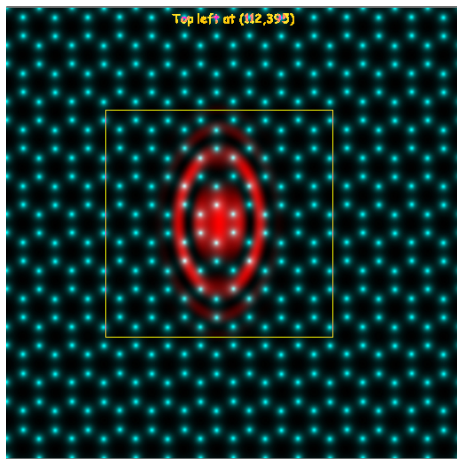


Figure: Probe affected by 2 fold astigmatism.

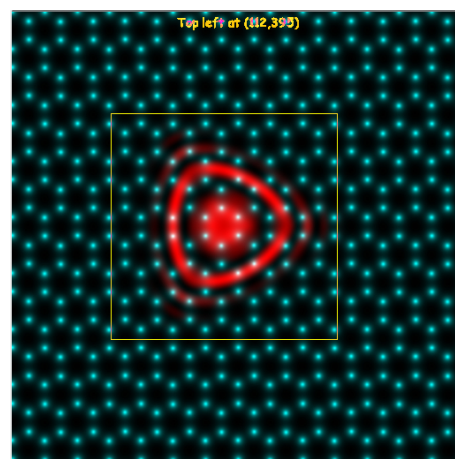


Figure: Probe affected by 3 fold astigmatism.

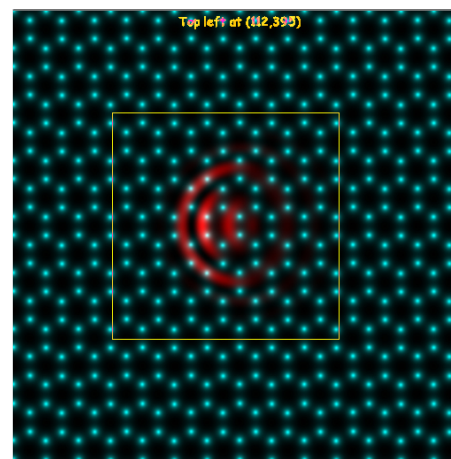


Figure: Probe affected by coma.

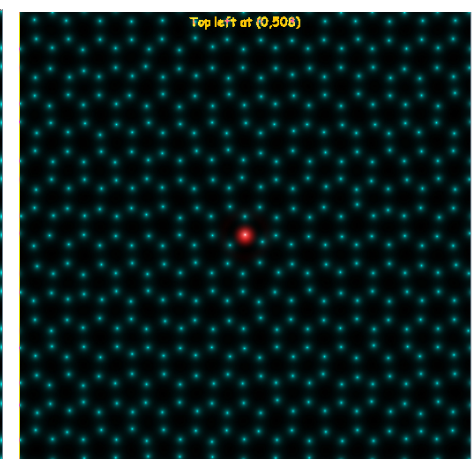


Figure: Corrected probe (best defocus).

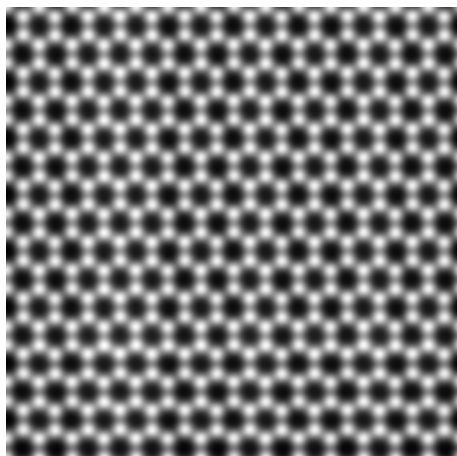


Figure: HAADF projected potential approximation.

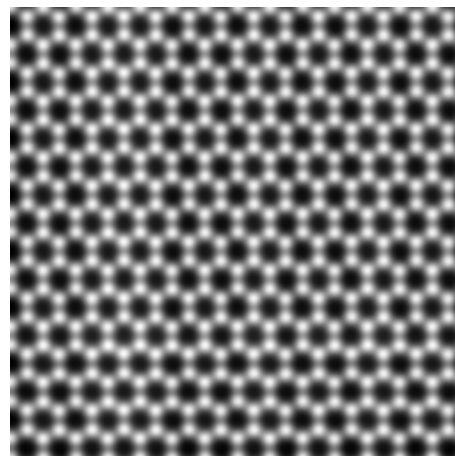


Figure: HAADF multislice calculation (simple).

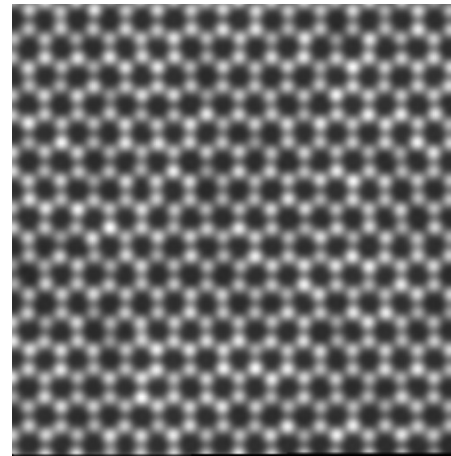


Figure: Frozen phonons 5 configurations.

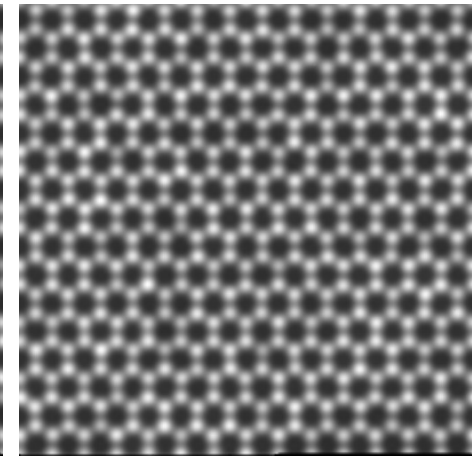


Figure: Frozen phonons 10 configurations.

Appendix 1: Dynamical theory of elastic scattering of high energy electron

We aim to understand in details **multiple elastic scattering** of electrons by crystals.

- ▶ High energy electron (eE).
- ▶ **Periodic** interaction potential $V(\vec{r})$.
- ▶ Time **independent** flux of incident electrons.

The **fundamental equation of electron elastic scattering** by a potential V_v [Volt] (positive inside a crystal) in the approximation of a stationary flux of electrons of a given energy eE is the **Schrödinger** equation¹⁸:

$$\Delta \Phi(\vec{r}) + \frac{2me}{\hbar^2} [E + V_v(\vec{r})] \Phi(\vec{r}) = 0$$

With a change of notation its is written as:

$$[\Delta + 4\pi^2 K_i^2] \Phi(\vec{r}) = -4\pi^2 V_v(\vec{r}) \Phi(\vec{r})$$

Where the wavevector $|\vec{K}_i|$ of the incident electrons is given by:

$$|K_i| = \frac{\sqrt{2meE}}{h}$$

and

$$m = \gamma m_0$$

¹⁸C. Humphreys, The scattering of fast electrons by crystals, Rep. Prog. Phys. **42** (1979) 1825-1887.

Schrödinger equation

The Laplacian $\Delta = \frac{\partial^2}{\partial x^2} + \frac{\partial^2}{\partial y^2} + \frac{\partial^2}{\partial z^2}$ is written as: $\Delta_\rho + \frac{\partial^2}{\partial z^2}$. As a result, $[\Delta + \dots]e^{2\pi i k_z z} \Psi(\rho; z)$ is given by: $[\Delta_\rho + \frac{\partial^2}{\partial z^2} + \dots]e^{2\pi i k_z z} \Psi(\rho; z)$.

Performing the z-differentiation:

$$\frac{\partial^2}{\partial z^2} e^{2\pi i k_z z} \Psi(\rho; z) = e^{2\pi i k_z z} \left[-4\pi^2 k_z^2 + 4\pi i k_z \frac{\partial}{\partial z} + \frac{\partial^2}{\partial z^2} \right] \Psi(\rho; z)$$

Inserting the last expression and dropping the term $e^{2\pi i k_z z}$:

$$\left[\Delta_\rho + 4\pi^2 (K_i^2 - k_z^2 + V(\rho; z)) + 4\pi i k_z \frac{\partial}{\partial z} + \frac{\partial^2}{\partial z^2} \right] \Psi(\rho; z) = 0$$

Since $K_i^2 = k_z^2 + \chi^2$:

$$\left[\Delta_\rho + 4\pi^2 \chi^2 + 4\pi^2 V(\rho; z) + 4\pi i k_z \frac{\partial}{\partial z} + \frac{\partial^2}{\partial z^2} \right] \Psi(\rho; z) = 0$$

Rearranging the last equation:

$$i \frac{\partial \Psi(\rho; z)}{\partial z} = -\frac{1}{4\pi k_z} \left[\Delta_\rho + 4\pi^2 \chi^2 + 4\pi^2 V(\rho; z) + \frac{\partial^2}{\partial z^2} \right] \Psi(\rho; z)$$

Fundamental equation

$$i \frac{\partial \Psi(\rho; z)}{\partial z} = -\frac{1}{4\pi k_z} [\Delta_\rho + 4\pi^2 \chi^2 + 4\pi^2 V(\rho; z) + \frac{\partial^2}{\partial z^2}] \Psi(\rho; z)$$

The term $|\frac{\partial^2 \Psi(\rho; z)}{\partial z^2}|$ being **much smaller** than $|k_z \frac{\partial \Psi(\rho; z)}{\partial z}|$ we drop it (this is equivalent to **neglect backscattering**).

Fundamental equation of **elastic scattering** of **high energy mono-kinetic electrons** with a potential within the approximation of **small angle scattering**:

$$i \frac{\partial}{\partial z} \Psi(\rho; z) = -\frac{1}{4\pi k_z} [\Delta_\rho + 4\pi^2 \chi^2 + 4\pi^2 V(\rho; z)] \Psi(\rho; z)$$

Time dependent Schrödinger equation \implies solution by many methods of quantum mechanics!

- ▶ The approximations of the fundamental equation are equivalent to assume that the **scattering potential is small compared to the accelerating potential** and that k_z varies only slightly with z . It is in fact a quite good approximation, since the mean crystal potential is of the order of $10 - 20 V$.
- ▶ **Electron backscattering** is neglected, the electron are moving forwards.
- ▶ The fundamental equation is actually equivalent to a **2-dimensional Schrödinger equation** ($\rho = \{x, y\}$) where z plays the role of time. The system evolution is **causal**, from the past to the future.

Fundamental equation in **Hamiltonian** form:

$$i \frac{\partial}{\partial z} \Psi = H \psi$$

where:

$$H = -\frac{1}{4\pi k_z} [\Delta_\rho + 4\pi^2 \chi^2 + 4\pi^2 V(\rho; z)] = H_o + \frac{4\pi^2 V(\rho; z)}{4\pi k_z}$$

A **fundamental postulate of quantum mechanics**¹⁹ says that the evolution operator obeys the equation:

$$i \frac{\partial}{\partial z} U(z, 0) = H(\rho; z) U(z, 0)$$

¹⁹R. Shankar, Principles of Quantum Mechanics (1994) Plenum Press, New York and London.

Causal evolution operator

$U(z, 0)$: **unitary operator** (the norm of $|\Psi\rangle$ is conserved), in general not directly integrable \implies **approximations**.

$U(z, 0)$ can be **directly integrated** only when $H(\rho; z)$ and $\frac{\partial}{\partial z}H(\rho; z)$ commute. In that case the general solution is²⁰:

$$U(z, 0) = e^{-i \int_0^z H(\tau) d\tau}$$

$H(\rho; z)$ and $\frac{\partial}{\partial z}H(\rho; z)$ commute when:

- ▶ $V(\rho; z)$ does not depend on z , i.e. $V(\rho; z) = V(\rho)$ (**perfect crystal**).
- ▶ $V(\rho; z)$ can be neglected (**free space propagation**).
- ▶ $H(\rho; z)$ is approximated by its potential term (**phase object**).

Three approximations are available in jems:

- ▶ **Multislice** method.
- ▶ **Bloch wave** method.
- ▶ **Howie-Whelan** column approximation.

²⁰A. Messiah, *Mécanique quantique* (1964) Dunod Paris.